Tohoku Univ., Sci. Rep., 2nd ser. (Geol.), v. 43, no. 1, p. 1–39,
17 text-figs., 9 tables, October 20, 1971

Detailed Study of the Sediments Recording the Matuyama-Brunhes Geomagnetic Reversal

Nobuaki Niitsuma*

ABSTRACT

The purpose of the present study is to find the relationship of a geomagnetic field reversal to the changes in a foraminiferal fauna and the sedimentary environments. A fossiliferous marine sedimentary section of the middle part of the Kokumoto Formation continuously exposed at Kamiyanagawa in the Boso Peninsula, Chiba Prefecture, Central Japan, was chosen for the investigation of the behaviour of the geomagnetic field during its reversal between the Matuyama and Brunhes Polarity epochs which took place around 0.69 m.y. ago. The behaviour of the geomagnetic field was established as to the inclination, declination and intensity of the Jn/J_R recorded in the sedimentary rocks. Along the same section, analyses were made on the grain-size of the sediments, oxygen isotope ratio in the planktonic and benthonic foraminiferal tests, and the faunal assemblages of the planktonic and benthonic foraminifers.

The intensity of the magnetic field fluctuated with a period of approximately 6700 years and did not disappear during the reversal. The migration of the virtual magnetic north pole at the magnetic field reversal between the Matuyama and Brunhes Polarity epochs occurred roughly along the meridian of 120° E long. in the period of 4700 years. In the same duration the depth of the sea water, under which the sediments accumulated, fluctuated within the range of 200–300 m with a period of approximately 7000 years. No particular relation between the magnetic field reversal and fluctuation of the water depth was recognized. The result of paleotemperature and faunal analyses of the foraminifers showed that the magnetic field reversal at the Matuyama Brunhes Polarity Epoch boundary may have been related to the changes in the circulation pattern of the upper watermasses which caused more influx of cold water into this area in the northwestern Pacific as compared with the period before the geomagnetic polarity change.

CONTENTS

LIST OF ILLUSTRATIONS

* Department of Earth Science, College of Arts and Sciences, Tohoku University, Sendai, Japan.

INTRODUCTION

Geomagnetic reversals during the last 5 million years have been recognized by magnetic measurements of volcanic rocks of known radiometric age (Cox *et al.*, 1963, 1967; Cox, 1968, 1969). The standard geomagnetic time scale has been extended to the records in sedimentary sequences from deep-sea cores (Opdyke *et al.*, 1966; Hays *et al.*, 1969), as well as those exposed on land (Nakagawa *et al.*, 1969, 1971; Niitsuma, 1970). The biostratigraphic studies of microfossils in deep-sea cores with the geomagnetic time control have made some authors to suggest that relation between the geomagnetic field reversals and the observed faunal appearances and extinctions exists (Opdyke *et al.*, 1966; Hays and Opdyke, 1967; Hays *et al.*, 1969). Others, however, (Waddington, 1967; Black, 1967; Harrison, 1968), after quantitatively estimating the effects of direct and/or indirect radiations from cosmic rays, solar flares and solar wind, have concluded that they can not be significant factors causing the appearance or extinction of marine species have if their amount increases during the reversals.

The appearance and extinction of some marine species may be caused by such biological changes that happen in an ecosystem such as changes in a part of the food chain, in

the ecologic position of the species, etc. They are intimately related to changes in the physical and chemical environments including the climate and circulatory systems in the ocean.

The present study aims to examine the relationships between geomagnetic reversals and changes in sedimentary environments with special reference to Foraminifera and to determine if any causal, whether relationships direct or indirect exist. A continuously exposed fossiliferous marine section has been chosen to see the behaviour of the magnetic field reversal between the Matuyama and Brunhes Polarity epochs that took place around 0.69 m.y. ago. Since the rate of sedimentation of the neritic sequence is much higher than those in the deep-sea, the geomagnetic records in detail the behavior of the magnetic field during the reversal. The rate of sedimentation has been estimated for this section using geomagnetic chronology (Nakagawa *et al.*, 1969), so that it is possible to estimate the amount of time which elapsed during the reversal and other related changes. Along with the geomagnetic measurements, the following analyses have been made. They are a sedimentological analysis of the sediments, paleotemperature measurements of planktonic and benthonic foraminiferal tests by means of oxygen isotopic ratio and faunal analyses of the benthonic and planktonic foraminiferal fauna.

ACKNOWLEDGMENTS

The writer wishes to express his deep gratitude to the following persons: Professors Kiyoshi Asano, Kotora Hatai and Jun-ichi Iwai, Tohoku University, for suggestions and reading the manuscript; Assistant Professor Yokichi Takayanagi, Tohoku University, for the suggestions on identification of planktonic Foraminifera; Doctor Hisao Nakagawa, Tohoku University, for the valuable suggestions on the stratigraphical problems, continuous encouragements and critical reviewing the manuscript; Doctor Taro Kanaya, Kanaya Paleontological Laboratory, for the valuable suggestions and discussions on the paleontological problems, continuous encouragements and critical reviewing the manuscript; Professor Yoshio Horibe, Tokyo University, for the guidance and suggestions in isotopic analysis, and reviewing the manuscript; Assistant Profesor Kazuo Kobayashi, Tokyo University, for suggestions and discussions on the paleomagnetic problems and reviewing the manuscript; Doctor Yasumochi Matoba, Akita University, for the discussion and suggestions on identification of benthonic Foraminifera; Doctor Neil D. Opdyke, Columbia University, for reviewing the manuscript; Professor Allan Cox, Stanford University, for reading the manuscript; Doctor Walfgang H. Berger, Kiel Univeristy, for the discussions and suggestions on the problems relating to the present study.

NOTE ON THE GEOLOGICAL HISTORY AND THE LATE CENOZOIC GEOMAGNETIC STRATIGRAPHY OF THE BOSO PENINSULA

The Boso Peninsula is situated in the southeastern part of the Kanto Region, central Japan (Fig. 1).

The stratigraphy of the Neogene and Pleistocene rocks exposed in the peninsula is summarized in Table 1, following the scheme by Nakagawa (1962).

The total thickness of the Nakahara and younger formations exceeds 6000 meters. They are all of marine origin. The series is continuous in sequence except for the sedimentary break between the Anno and Kurotaki formations; the hiatus is estimated to be equivalent to about 150 m thick sediments of the surrounding area. The marine Neogene and Pleistocene formations of the Boso Peninsula consist largely of alternations of siltstone and sandstone. They frequently intercalate pyroclastic layers by which detailed tephro-

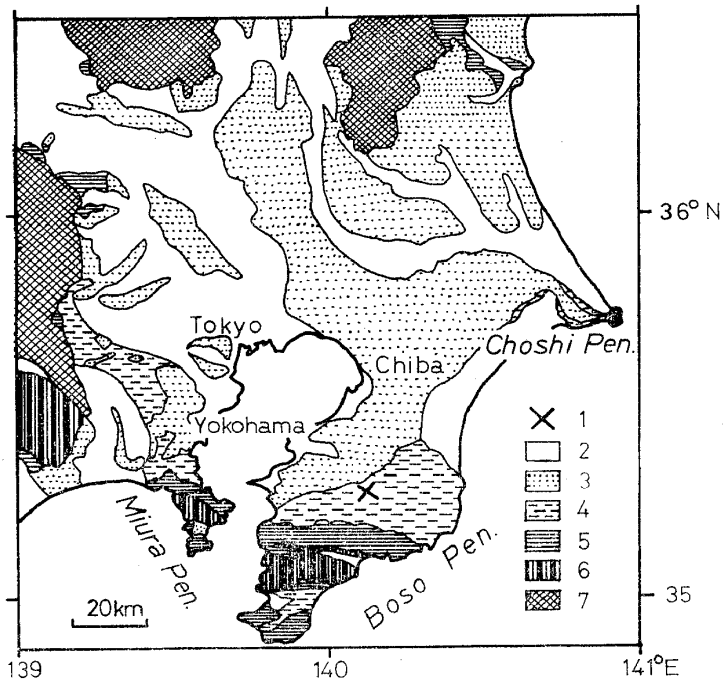

Fig. 1 Geologic sketch map of Kanto Region, Central Japan.
1: Sampling position 2: Younger sediments 3: Narita Group
4: Akimoto and Seki groups 5: Toyooka and Sakuma groups
6: Hota and Mineoka groups 7: Pre-Tertiary rocks

Table 1 Stratigraphy of Neogene and Pleistocene rocks exposed in the Boso Peninsula.

Narita Group	Kioroshi Formation Kamiiwahashi F. Semata F. Yabu F. Jizodo F. Kasamori F. Mandano F. Chonan F.
(conformity)	
Akimoto G.	Kakinokidai F. Kokumoto F. Umegase F.
(conformity)	
Seki G.	Otadai F. Kiwada F. Kurotaki F.
(unconformity)	
Toyooka G.	Anno F. Kiyosumi F.
(conformity)	
Sakuma G.	Amatsu F. Nakahara F.
(unconformity)	
Hota G.	
(fault)	
Mineoka G.	

chronology of the sedimentary rocks has been established (Mitsunashi *et al.*, 1959, 1961). The marine formations are fossiliferous and a number of paleontological and biostratigraphical studies have been made dealing with molluscs (e.g. Hatai, 1958; Ogose, 1961) and

benthonic and planktonic Foraminifera (e.g. Asano, 1938; Saito, 1963; Aoki, 1968).

The Mineoka and Hota groups are distributed along the axis of the anticlinal zone of the southern part of the Boso Peninsula (Fig. 1), and are intensely faulted and folded and intruded by basic and ultrabasic igneous rocks. The Nakahara Formation, unconformably overlying the Hota Group, is also folded and faulted in the anticlinal zone. The Amatsu Formation directly covers the Hota Group and together with the overlying formation is gently folded. The Nakahara Formation includes a horizon correlated with the *Globigerinatella insueta/Globigerinoides bisphericus* Subzone (Saito, 1963), and yielded larger Foraminifera as *Amphistegina, Lepidocyclina, Miogypsina*, as well as Mollusca and other fossils (Hanzawa, 1931). The Kurotaki and younger formations dip homoclinally north-westwards. The Kioroshi Formation, the youngest of the Narita Group, is subhorizontal and is distributed not only in the peninsula but also widely in the central part of the Kanto Region. The Kioroshi Formation is conformably overlain by the clay of volcanic ash origin of the Shimosueyoshi Volcanic Ash covering the Shimosueyoshi Terrace formed during the last high sea-level and warm water temperature stage in the Late Pleistocene (Nakagawa, 1965).

In the later phase of the accummulation of the Toyooka Group, a zone with axis trending in WNW-ESE direction had been anticlinarlly uplifted in the preceeding marine sedimentary basin of the southern part of the Kanto Region, in which the Toyooka Group was deposited. In the Kazusa Sedimentary Basin developed succeedingly on the north of this anticlinal zone, thick marine Pliocene and Pleistocene sediments of the Seki and Akimoto groups were accummulated. The marine sedimentation appears to have been continuous in the central area even during the later transformation of the trough-shaped Kazusa Sedimentary Basin into the doubly pluging synclines called the Kanto Tectonic Basin, in which the Narita Group was deposited.

At attempt was once made by Kawai (1951) to measure the Natural Remanent Magnetization (NRM) of the samples from the Late Cenozoic marine sediments of the Boso Peninsula. Recently, Nakagawa, Niitsuma and Hayasaka (1969) succeeded in measuring the Detrital Remanent Magnetization (DRM) of siltstones in the sequence from the Amatsu up to the Kioroshi formations in the peninsula (Fig. 2). The results correlates well with the scheme of geomagnetic field reversals given by Cox (1969).

Correlating with the geomagnetic scheme of Cox (1969), Nakagawa *et al.* (1969) were able to identify the boundary between the Brunhes and Matuyama Polarity epochs in the middle part of the Kokumoto Formation, that between the Matuyama and Gauss in the lower part of the Umegase Formation, and that between the Gauss and Gilbert in the lowermost part of the Otadai Formation.

Comparison of the paleomagnetic and microbiostratigraphic sequence between the Boso Peninsula and south Italy (Nakagawa, Niitsuma and Elmi, 1971) suggests that the time equivalent of the boundary between the Pliocene and the Calabrian in le Castella area is likely to be found in the upper part of the Umegase Formation.

The boundary between the Pliocene and Miocene is now interpreted to be the unconformity between the Anno and Kurotaki formations, if we accept the correlation between the planktonic Foraminifera zones and geomagnetic polarity sequence presented by Berggren (1969).

DEPOSITIONAL CONDITION AND RATE OF SEDIMENTATION OF SILTSTONE

Pliocene and Pleistocene marine formations in the Boso Peninsula consist mostly of alternations of sandstone and siltstone. Thin layers of tuff are intercalated in the

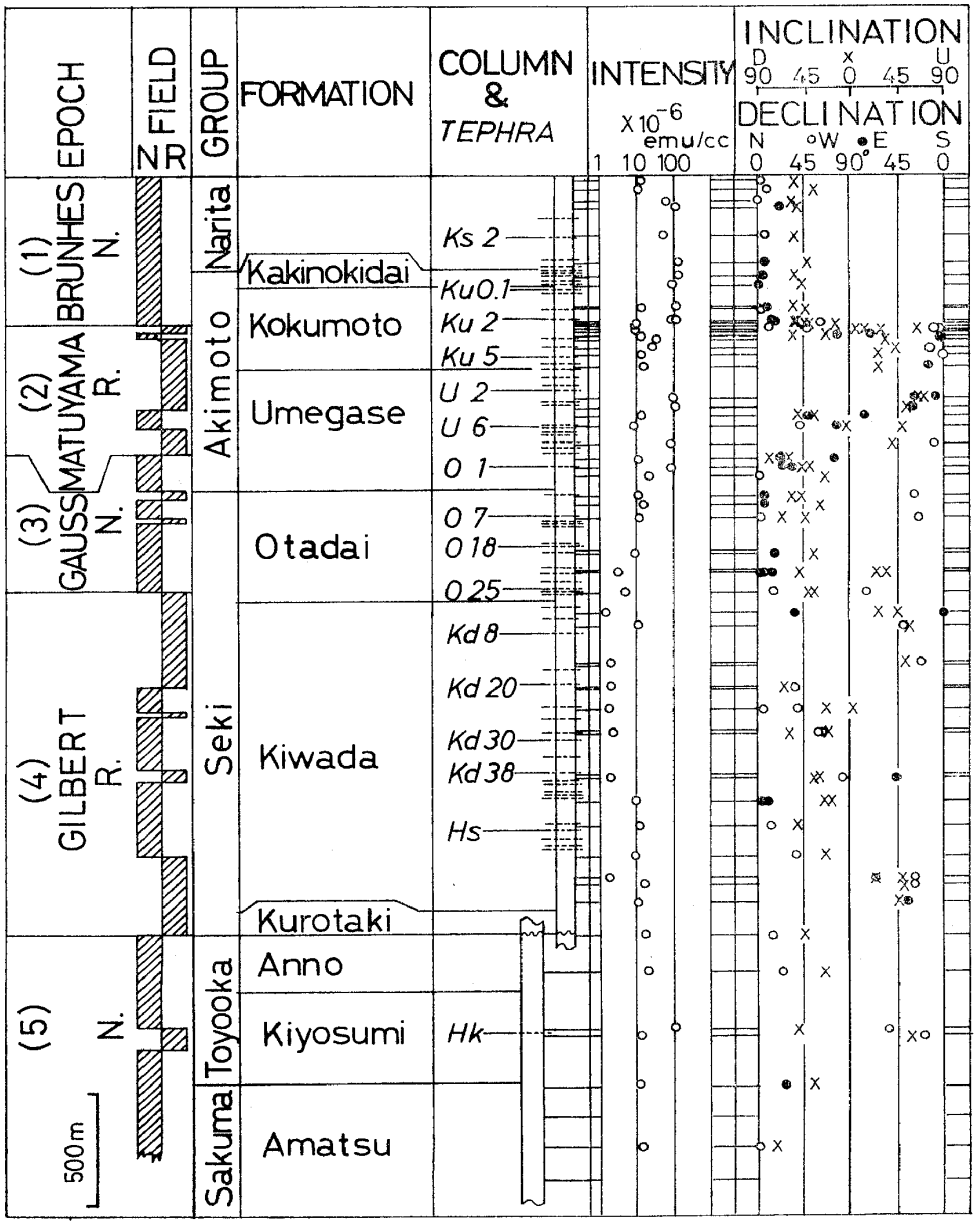

Fig. 2 Late Cenozoic geomagnetic stratigraphy in the central and northern parts of the Boso Peninsula.

The original record (Nakagawa *et al.*, 1969), particularly of those below the Gauss has been re-interpreted to divide them into two magnetic polarity epochs (Niitsuma, 1971) rather than four as was originally done.

siltstones and they are frequently useful as keys in tracing stratigraphic levels over widely separated sections. For example, a set of three 10–20 cm thick layers of tuff, named Ku 2 is intercalated in the middle part of a 150 m thick siltstone bed (Fig. 2) that forms a part of the alternation of siltstone and sandstone of the Kokumoto Formation, in the Yoro Valley of the peninsula. The Ku 2 can be traced for distance of 45 km from the west to east coasts in the central part of the Boso Peninsula (Mitsunashi *et al.*, 1959; 1961), its position relative to the Matuyama / Brunhes boundary has already been ascertained in the previous study (Nakagawa *et al.*, 1969).

The thickness of the siltstones interbedded with tuff layers, as well as the thickness of each tuff layer changes little in the western part of the Boso Peninsula, therefore it is inferred that the rate of sedimentation was mostly constant in this area. The depositional surfaces of the tuff layers are always flat and parallel with the bedding plane. These facts are taken as indication that the tuffs had been deposited on the horizontal sea bottom under a calm condition. Disturbance by burrowing organisms is sometimes observed along the upper surface of tuff layers, but the disturbance does not extend more than a few centimeters in depth, suggesting that the siltstones in which the tuffs are intercalated were deposited also on a horizontal plane at a constant rate of sedimentation under a calm condition. This observation holds true in this study (see Fig. 6).

Hirayama and Suzuki (1968) reported that there are changes in thickness of each members in the alternations of sandstone and siltstone of the Otadai Formation in an interval (3–5 m thick) between two key tuffs, O_7 and K_3. On the basis of the observations made on this interval in the central part of the Boso Peninsula over the distance of 45 km, they found that the thickenss of each siltstone bed changes a little; each sandstone bed, however, thickness as much as twice in the central part of the Boso Peninsula. This difference in the lateral changes of thickness between sandstone and siltstone seemed to suggest that the mechanisms of their deposition may have been different. The alternation beds in the Kokumoto Formation is of the same type as the Otadai Formation. In order to bear this possibility out, the sandstone layers alternating with siltstone were examined particularly along the magnetically studied section at Yanagawa (Fig. 5). The thickness measured in that section shows a logarithmic normal distribution, which suggest that the deposition of sandstone layers were governed by a single cause (Fig. 3). The sandstones were studied further as to their texture by means of the automatic grain-size analyser, made specifically by the present author (Niitsuma, 1971). The grain-size distribution patterns observed for sandstones thicker than 100 cm are constantly unimodal, with the maximal at 2.6ϕ (Fig. 4). The pattern coincide with what have been found for modern sands along the near shore zone of 10–13 m in depths both in Mutsu Bay and the northern part of the Pacific coast of Japan (Niitsuma and Mekata, 1971a, b). The grain-size dist-

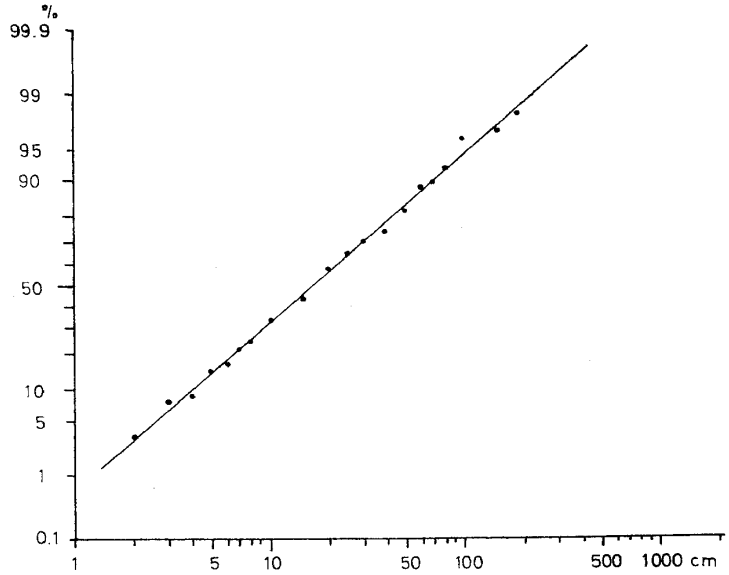

Fig. 3 Thickness in logarithmic scale of sandstones in the alternation of sandstone and siltstone of the Kokumoto Formation, plotted on probability paper.

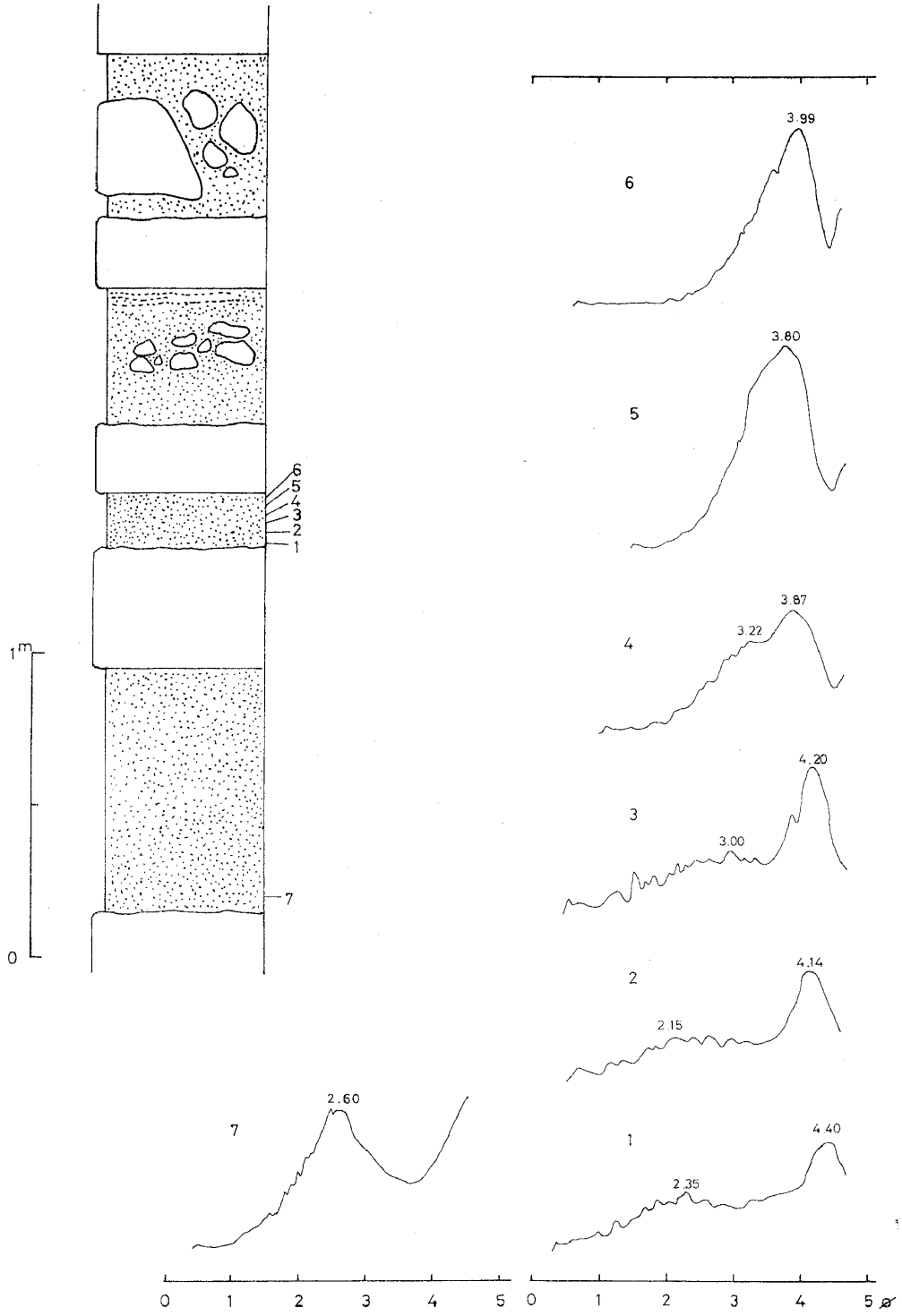

Fig. 4 Frequency curves of grain-szie in sandstone alternating with siltstone.

ribution in the sandstone layers less than 100 cm thick, however, varies in parts, changing gradually from the lower part to the upper part (Fig. 4). That type of the pattern has not so far been found among the modern sand of Mutsu Bay and the northern part of the Pacific coast of Japan. The results of sedimentological analysis suggest that the sandstone was deposited under a special hydrodynamic condition. Meanwhile the surface of the

siltstone in the alternation is usually sculptured by the overlying sandstone and soft siltstone blocks are often included in the sandstone. It is obvious that the sands were once deposited in the neritic zone and then flowed down as so-called turbidity currents, during which courses the underlying siltstone was sculptured to be incorporated as soft siltstone blocks and as silt particles into the sand flow. Their deposition are instantaneous on the sea bottom, interrupting the deposition of the siltstones accummulated on the horizontal plane at a nearly constant rate of sedimentation under a calm condition.

The rate of sedimentation at the horizon near the boundary between the Matuyama and Brunhes epochs in the Kokumoto Formation was estimated in average to be 57 cm/ 1000 years (Nakagawa *et al.*, 1969). If the sandstones were formed instantaneously as is suggested above, the siltstone must have accummulated at a much slower rate. The ratio of the total thickness of the sandstones to siltstones in the sequence is 1.00:1.09 from the columnar section along the Yoro Valley (330–690 m by Mitsunashi *et al.*, 1961). The rate of sedimentation for siltstone in the sequence could be calculated at 29.7 cm/ 1000 years $\left(=57\times\frac{1.09}{1.09+1.00}\right)$ on the assumptions that (i) the rate of sedimentation for siltstone was constant, and (ii) the sandstone in the sequence was deposited instantaneously.

A rate of sedimentation for the siltstone at 29.7 cm/ 1000 years is larger than, for instance 0.75–1.13 cm/ 1000 years for red clay (Ninkovich *et al.*, 1966) and 1.98 cm/ 1000 years for *Globigerina* ooze (Oba, 1969) in the deep sea sediments. If this figure is correct, the 3.5 cm thick test piece measured in the present work represents an average period of 118 years, a duration short enough for examination of secular variation of the earth's magnetic field.

SAMPLES

It has already been known by the work by Nakagawa *et al.* (1969) on the basis of the measurements made for samples taken at 25 m stratigraphic intervals, that the boundary between the Matuyama and Brunhes Magnetic Polarity epochs lies in the middle part of the Kokumoto Formation: the interval over the boundary can be narrowed down to the levels between 170–200 m of the Kokumoto Formation in the columnar section along the Yoro Valley presented by Mitsunashi *et al.* (1959). This stratigraphic interval supposed to include the boundary was traced in the field by means of a set of key tuffs to the sequence showing similar lithology along a tributary of the Yoro Valley in the valley of Yanagawa (Fig. 5), where the condition for detailed continuous sampling is best suited.

Since the present study involves the correlation of results obtained by various lines of studies, a control is necessary as to the quantity and relative position of each sample used in laboratory studies and measurements. Furthermore, an oriented sample normal to the bedding plane is required for the paleomagnetic measurements. For this reason samples were taken in the field by directly coring the rocks at the outcrops. The Macandrill with Mac–35A type engine of McCullogh Co. was used with two kinds of bits: a diamond bit of 35 mm in inner diameter and a metal-crown bit of 150 mm in inner diameter with core tubes 350 mm and 200 mm in length, respectively. In both cores water for sweeping the cuttings was supplied by means of water-swivel. The fresh part of the sedimentary rocks was cored vertically to their bedding plane.

The sampling from the Yanagawa section was made in three steps. Firstly, siltstone samples were taken at every one meter through the stratigraphic interval, 40 m thick (Fig. 5). The samples from KM 71–97 represent in an ascending order a 20 m thick sequence below the supposed boundary traced from the one found by the previous work (Nakagawa *et al.*, 1969); those from KM 11–23 represents, in as ascending order a 20 m

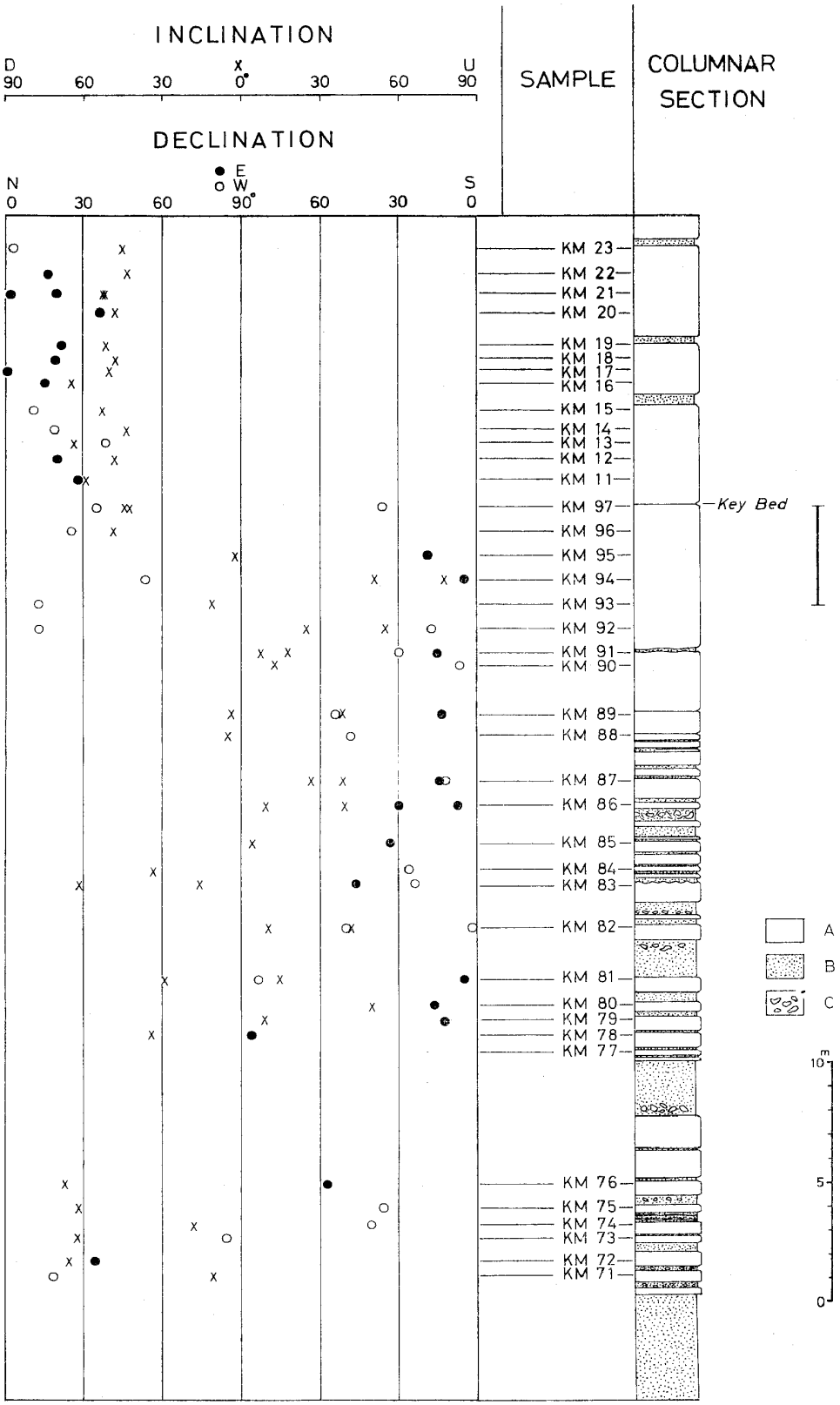

Fig. 5 Lithology and the results of paleomagnetic measurements from the Yanagawa section.
A: siltstone, B: sandstone, C: siltstone gravel

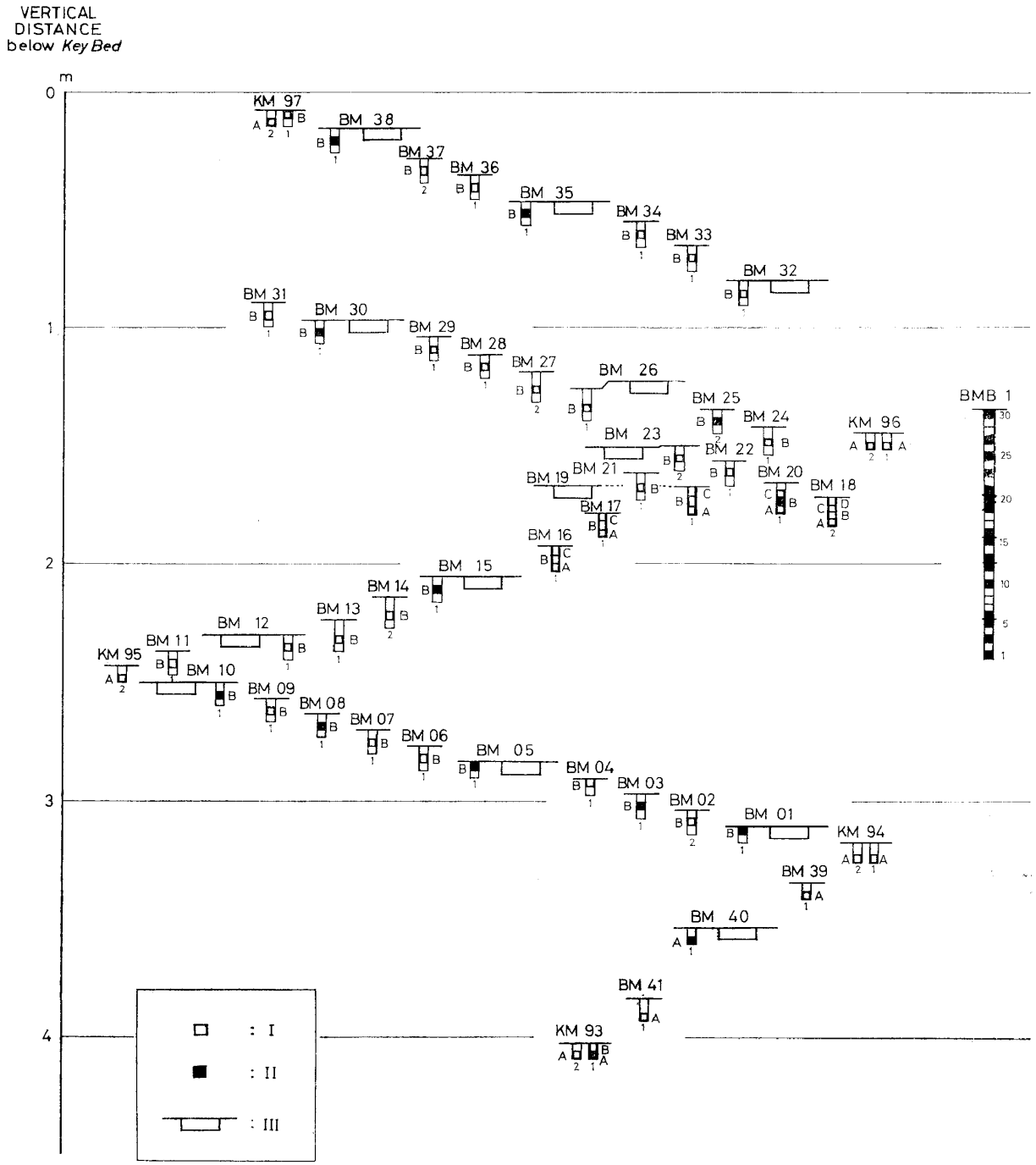

Fig. 6 The position of samples taken for the detailed study of the Matuyama-Brunhes boundary.
I: sample for paleomagnetic and sedimentological study
II: sample for paleomagnetic, sedimentological and foraminiferal study
III: sample for study of oxygen isotope

thick sequence above the supposed Matuyama and Brunhes boundary. At each stations, two cores were taken normal to the bedding plane, diameter and length being 35 mm and 120 mm, respectively. By the paleomagnetic measurements of these samples, the boundary was narrowed down further to exist between KM 95 and KM 96.

For the second steps for more detailed sampling about the boundary, samples were

taken at every 10 cm (BM 01–38) from the interval between KM 93 and KM 97 (Fig. 6). They consist of three cores, two cores of 35 mm in diameters and 120 mm in length, and another core of 150 mm in diameter and 50 mm length, taken at each site.

Moreover, the just boundary was crossed by a longer core (100 cm in length, 35 mm in diameter) taken to be continuous at the site (a series BMB 101–130).

Through these processes, the change of polarities representing the Matuyama and Brunhes boundary in the Yanagawa section was found, its position being 150 cm stratigraphically below the key tuff, a fine tuff layer 10 cm thick.

The samples were used in the following ways. Paleomagnetic measurements were made on 35 mm thick cylinders cut from 35 mm diameter cores. After the measurement, the test piece was cut longitudinally into three pieces; one half was for preservation, and one quarter for the foraminiferal studies. The samples taken by a 150 mm bit were used for collecting samples large enough to yield sufficient foraminiferal tests for oxygen isotope analysis.

EARTH'S MAGNETIC FIELD DURING REVERSAL

The method of measurement of DRM in the present work is almost the same as that described in Nakagawa *et al.* (1971). After the partial demagnetization, the direction and intensity of the remanent magnetization was measured at every 30° around three axes of the sample with the astatic-type magnetometer of the sensitivity of 5×10^{-8} Oe/mm. Each specimen was demangnetized in the alternation field of 90 Oersted to remove the unstable secondary components. The demagnetization was achieved with an apparatus similar to that described by Doell and Cox (1967), consisting of a tumbler rotating within an alternating field coil in nonmagnetic space provided by two pairs of Helmholz coils. All numerical values obtained from the measurement were processed by an electronic computer, NEAC 2200, Model 500, at the Computer Center of the Tohoku University (see Appendix). Numerical analysis of the data indicates that the measured values can be well approximated by a magnetic dipole so that the direction and intensity of the remanent magnetization thus determined are sufficiently reliable.

The result of measurements for stratigraphic intervals of 1 m (Fig. 5) shows that northward declinations and downward inclinations of DRM prevail in the part above the key tuff indicating that they are of normal magnetic polarity. Below the key tuff, the declinations were southward and the inclinations upward, therefore they are of reversed magnetic polarity (Table 2).

The results of measurements for the sequences of 4m below the key tuff (Fig. 7, Table 3) show that the declination changed abruptly from southward to northward at a level of 170 cm below the key tuff; the inclination changed gradually from 40° upward to 40° downward between 240 cm below the key tuff and 100 cm below the key tuff. The inclination moved through the horizontal at 200 cm to 90° downward at 170 cm below the key tuff. The positions of virtual magnetic pole are calculated from these values and are plotted in Fig. 5. It seems to show that the virtual magnetic north pole migrated from the geographic south pole to the north pole along the meridian of 120° E.

The ratio of the intensity of DRM after AC-demagnetization by 90 Oe, Jn, to that of isothermal remanent magnetization after application of a direct field of 5000 Oe, J_R, is measure and plotted in Fig. 8. Although the intensity of the depositional remanent magnetization is not necessarily proportional to the intensity of the ambient field (Nagata, 1961), the values Jn/J_R may still be useful as an indication of the paleomagnetic intensity. Minima of Jn/J_R were recognized at the horizons 400, 235, 180 and 10 cm below the key tuff. The minimal ratios at the horizon 235 cm below the key tuff occurred at the beginning of

Table 2 Paleomagnetic measurements obtained for Yanagawa samples.

Sample	Declination (+ W, - E)	Inclination (+ U, - D)	Standard deviation	Intensity 10^{-5}emu/cc
KM 23	N+ 3.0± 2.6	-45.3± 3.2	0.08,0.12,0.09	4.48
22	N-16.6± 6.2	-43.4± 6.2	0.10,0.06,0.09	3.46
21	N- 1.9± 0.6	-52.2± 5.0	0.04,0.05,0.23	6.05
	N-19.5± 5.3	-52.4± 3.0	0.05,0.07,0.07	7.15
20	N-36.1±10.8	-48.4± 8.2	0.11,0.11,0.10	7.85
19	N-21.4± 6.1	-51.7± 1.9	0.11,0.09,0.24	5.59
18	N-19.3± 8.6	-47.9± 8.3	0.07,0.05,0.06	4.57
17	N- 0.8± 7.5	-50.3±11.5	0.35,0.07,0.06	3.34
16	N-15.2±15.5	-64.8±10.6	0.06,0.15,0.11	3.65
15	N+10.7± 1.1	-52.6± 6.3	0.07,0.11,0.15	3.59
14	N+18.9± 3.5	-43.4± 1.7	0.06,0.14,0.09	3.50
13	N+38.8± 1.0	-63.1± 3.3	0.08,0.06,0.09	2.34
12	N-20.0± 7.2	-48.1± 7.1	0.16,0.05,0.16	3.46
11	N-28.1± 8.9	-59.5± 4.4	0.08,0.09,0.07	4.90
97	S+36.1±24.7	-44.7±37.7	0.18,0.55,0.23	0.73
	N+34.7± 0.2	-42.4±19.3	0.34,0.16,0.63	0.92
96	N+25.4±15.7	-48.7± 1.2	0.14,0.16,0.14	1.41
95	S-18.9± 8.0	- 2.4± 1.4	0.10,0.18,0.03	2.82
94	S- 4.8± 7.2	+50.9± 5.7	0.07,0.12,0.15	1.80
	N+53.3±11.4	+76.9± 3.3	0.17,0.13,0.78	2.33
93	N+12.6± 5.4	-11.5±29.7	0.21,0.32,0.17	0.96
92	N+12.7±18.6	+35.5± 4.1	0.16,0.35,0.11	2.60
	S+17.2±18.0	+24.7± 5.2	0.16,0.17,0.04	4.16
91	S-15.7±25.0	+ 7.2±27.9	0.16,0.32,0.09	1.26
	S+29.5± 6.7	+17.7± 3.0	0.07,0.06,0.06	4.48
90	S+ 6.4± 0.5	+12.3± 9.8	0.22,0.07,0.11	2.86
89	S+52.8±14.9	- 3.9±10.7	0.32,0.14,0.16	2.28
	S-13.5± 8.1	+38.1±24.1	0.13,0.09,0.04	2.37
88	S+48.6±33.2	- 4.9± 1.9	0.39,0.53,0.68	0.54
87	S+12.5±16.7	+38.9±11.6	0.08,0.22,0.15	1.44
	S-14.8±39.1	+27.2±13.3	0.14,0.10,0.03	2.82
86	S-29.8± 0.2	+ 9.1± 6.8	0.18,0.15,0.08	1.82
	S- 7.7± 1.0	+39.6±14.2	0.10,0.13,0.17	3.34
85	S-33.6±68.2	+ 3.8±11.9	0.29,0.82,0.06	1.85
84	S+26.2± 4.6	-33.5± 2.7	1.34,0.10,0.17	1.20
83	S-45.8±25.0	-61.9± 8.8	0.20,0.33,0.14	1.48
	S+23.8±19.3	-15.8± 4.6	1.25,0.25,0.07	2.07
82	S-49.5±10.5	+10.4±22.5	0.33,0.34,0.12	0.83
	S+ 1.8±93.2	+40.2± 0.5	0.45,0.03,0.11	1.18
81	S- 4.7±87.3	-29.2±39.7	1.53,0.43,0.27	0.20
	S+83.4±98.9	+14.2±46.6	0.24,0.38,0.11	1.37
80	S-16.3± 0.8	+49.8±12.4	0.06,0.16,0.20	2.30
79	S-12.5± 6.8	+ 8.8± 9.9	0.15,0.31,0.07	2.94
78	S-86.7± 1.7	-34.6±45.1	0.20,0.25,0.18	3.68
76	S-57.4±39.2	-67.1±22.7	0.10,0.13,0.12	3.51
75	S-35.6±83.2	-62.1±14.6	0.21,0.38,0.12	3.54
74	S+40.6±22.3	-18.1± 5.1	0.76,0.37,0.08	2.15
73	N+84.7±19.4	-62.6± 5.1	0.25,0.26,0.14	2.16
72	N-34.5±36.3	-65.3±20.6	0.09,0.18,1.66	2.26
71	N+18.3± 3.9	-10.8± 5.6	0.59,0.41,0.09	1.87

the magnetic field reversal shown by inclinations. During the geomagnetic field reversal was recognized between the horizons 240 cm and 100 cm below the key tuff, the intensity apparently remained in smaller values. As Fig. 7 indicates in a general tendency, the intensity of the paleomagnetic field oscillated periodically, with a period represented by 200 cm in thickness of sediments. The maximum values of the Jn/J_R are about three times larger than the minimum values. During a polarity change, the intensity of the field decreased, the magnetic field, however, never vanished as was suggested by the oriented DRM (Fig. 8).

At the two horizons of minimal intensity, 400 and 100 cm below the key tuff, the

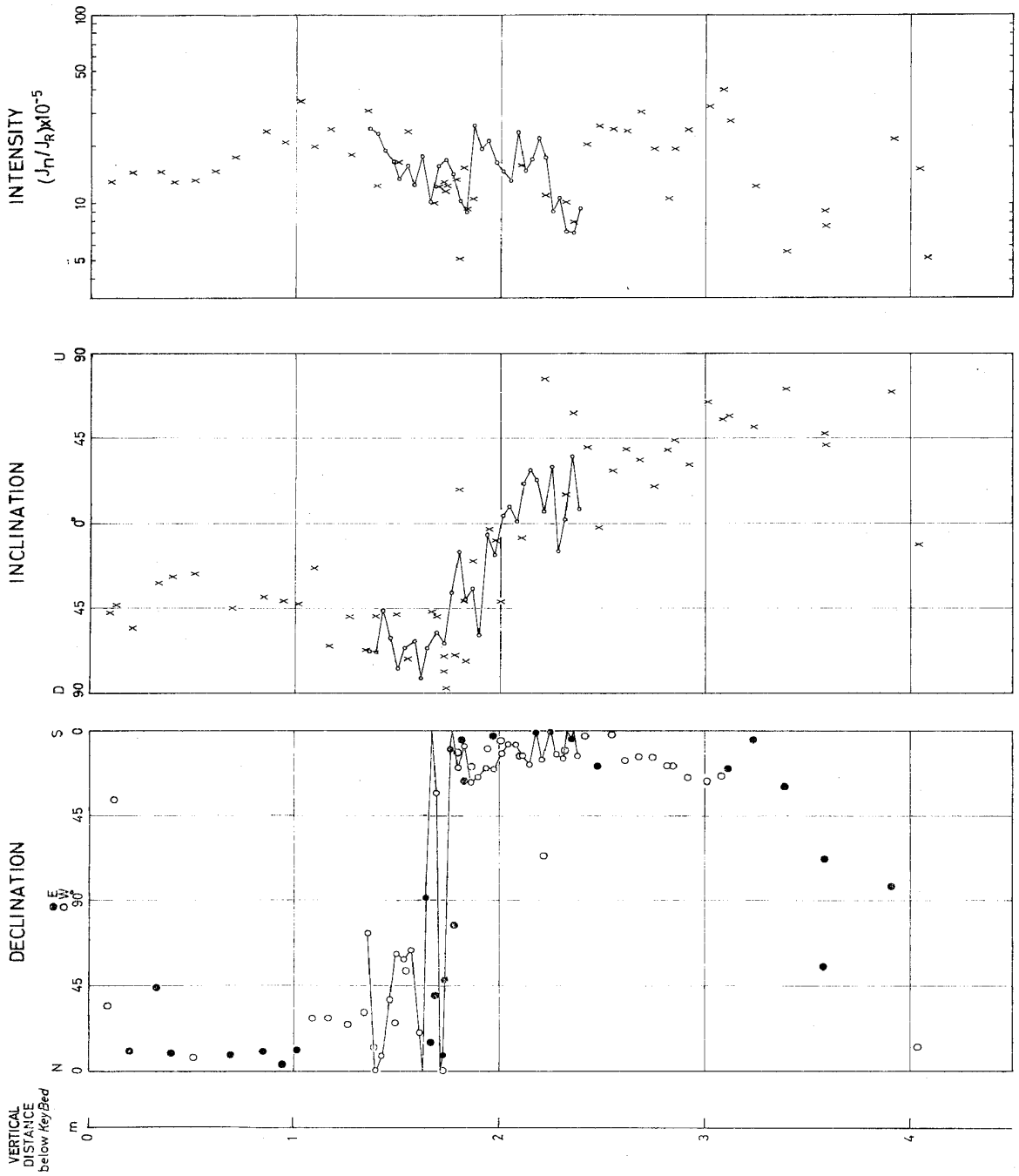

Fig. 7 Results of paleomagnetic measurements.

Each plot represents a sample; those taken from a single continuous core are connected by lines. J_n/J_R is a ratio of the intensity of DRM after AC-demagnetization by 90 Oe to the intensity of isothermal remanent magnetization after application of a direct field of 5000 Oe.

Table 3a Paleomagnetic measurements obtained for the Matuyama-Brunhes boundary.

Sample	Declination (+ W, - E)	Inclination (+ U, - D)	Standard deviation	Intensity $\times 10^{-5}$ emu/cc	J_n/J_R $\times 10^{-5}$
KM971B	N+34.7± 0.2	-42.4±19.3	0.34,0.16,0.63	0.92	12.8
972A	S+36.1±24.7	-44.7±37.7	0.18,0.55,0.23	0.73	
BM361B	N-10.6±17.3	-55.2± 8.6	0.12,0.12,0.18	1.07	14.4
372B	N-44.0±33.0	-31.9± 6.9	0.29,0.22,0.09	1.22	14.6
361B	N- 9.4±17.6	-28.7± 8.3	0.35,0.28,0.11	1.13	12.8
351B	N+ 7.1±10.2	-26.8± 4.1	0.27,0.09,0.19	1.12	13.1
331B	N- 8.4±17.2	-45.6±12.1	0.22,0.13,0.14	1.66	17.6
321B	N-10.3± 5.4	-39.2± 7.2	0.09,0.14,0.12	3.06	23.5
311B	N- 3.6±13.7	-41.4± 3.4	0.11,0.14,0.07	2.31	20.5
301B	N-10.9± 6.7	-42.8± 6.4	0.07,0.07,0.02	7.83	34.3
291B	N+28.0± 1.5	-23.9± 2.0	0.29,0.21,0.06	1.96	19.5
281B	N+27.9± 9.1	-65.1± 0.9	0.08,0.10,0.08	2.00	24.2
272B	N+24.8± 1.7	-49.7± 4.6	0.19,0.15,0.14	1.58	17.6
261B	N+30.9± 5.5	-67.4± 1.0	0.15,0.16,0.14	2.75	31.0
252B	N+12.6± 6.6	-49.4± 5.7	0.28,0.10,0.14	0.87	12.2
KM961A	N+25.4±15.7	-48.7± 1.2	0.14,0.16,0.14	1.41	16.4
BM252B	N+52.9±14.0	-72.2± 5.3	0.13,0.16,0.13	2.71	23.9
211B	N-15.1±18.6	-47.0± 5.4	0.22,0.25,0.06	1.51	9.7
191C	N-40.1±34.9	-49.9±14.3	0.24,0.23,0.27	1.61	12.0
201B	N+ 0.2±18.9	-70.8± 7.7	0.34,0.20,0.11	1.85	12.8
182D	N+38.8±24.9	-79.1±19.2	0.10,0.31,0.39	1.69	11.5
181B	N-48.7±66.5	-87.4± 3.8	0.23,0.24,0.51	1.32	12.4
191A	N-77.0±58.7	-69.7±15.6	0.17,0.15,0.42	1.24	13.3
171C	S+11.5± 2.1	+17.8±14.5	0.22,0.27,0.12	0.50	5.03
162A	S- 4.4± 0.8	-41.6± 1.0	0.14,0.13,0.10	1.42	15.3
171B	S-26.2±47.9	-73.6± 8.8	0.21,0.09,0.11	0.91	9.3
171A	S+18.5±12.6	-20.3± 8.1	0.18,0.19,0.13	0.91	10.4
161A	S+ 5.0± 0.3	-41.7± 8.9	0.16,0.22,0.09	0.83	
151B	S+12.8± 9.0	- 8.0± 4.2	0.10,0.23,0.08	1.89	15.8
142B	S+65.9±95.3	+75.6± 8.7	0.23,0.18,0.09	1.39	10.9
131B	S+10.6±16.8	+15.1± 5.1	1.54,0.17,0.08	0.93	10.1
121B	S- 2.3±14.4	+57.8± 2.0	0.49,0.11,0.35	0.89	7.9
111B	S+ 2.4± 1.5	+40.0± 6.2	0.34,0.22,0.08	1.70	20.0
KM952A	S-18.9± 8.0	- 2.4± 1.4	0.11,0.18,0.03	2.82	25.3
BM1013	S+ 2.0± 4.6	+27.7± 2.2	0.10,0.11,0.09	2.83	24.5
0913	S+15.4± 2.8	+39.0± 2.8	0.13,0.07,0.08	2.77	23.9
0813	S+13.9±16.2	+33.4± 9.4	0.15,0.04,0.24	3.72	30.4
0713	S+13.9± 1.7	+19.5± 1.6	0.10,0.05,0.08	3.18	19.1
0613	S+18.6±22.2	+38.8±13.1	0.15,0.14,0.07	2.04	10.6
0513	S+13.4± 7.1	+44.4± 7.2	0.11,0.06,0.10	3.27	19.2
0413	S+25.1± 5.6	+30.9± 2.6	0.25,0.09,0.06	3.45	24.4
0313	S+26.7±19.7	+64.1±10.4	0.13,0.10,0.32	4.85	32.8
0223	S+24.0± 8.4	+54.8± 3.7	0.12,0.17,0.22	3.05	40.2
0113	S-19.9± 7.2	+56.5± 1.5	0.13,0.10,0.15	3.67	27.0
KM941A	S- 4.8± 7.2	+51.0± 5.7	0.07,0.12,0.15	1.80	12.4
BM391A	S-29.5± 6.3	+71.4± 5.2	0.26,0.28,0.14	0.85	5.57
401A	S-68.2±98.3	+47.5± 0.7	0.38,0.12,0.14	1.76	9.2
402A	N-54.9±18.1	+41.5± 5.5	0.24,0.16,0.14	1.46	7.68
411A	S-82.9± 0.2	+69.8± 0.3	0.17,0.09,0.63	3.42	22.2
KM931B	N+12.6± 5.4	-11.5±29.7	0.21,0.32,0.17	0.96	5.19

declination varied greatly, though the inclination remained approximately the same. Such behavior of geomagnetic field has once been reported by Petorova (1965) as the behavior of "step I". The position of the virtual magnetic pole calculated from the horizons of the minimum intensity drifted along the meridians of 180°, 120° and 90° of east longitude at horizons 400 cm, 200 cm, and 10 cm below the key tuff, respectively. The drift of the virtual pole may be caused by the increase of the proportion of non-dipole moment in the total geomagnetic field caused by the main dipole moment decreasing at those horizons.

The duration of the magnetic field reversal can be calculated under the assumption that the rate of sedimentation is uniform at a magnetically dated stratigraphic interval.

Table 3b Paleomagnetic mesurements obtained for the Matuyama-Brunhes boundary. (continuous core)

Sample	Declination (+ W, - E)	Inclination (+ U, - D)	Standard deviation	Intensity $\times 10^{-3}$ emu/cc	J_n/J_R $\times 10^{-3}$
EMB130	N+72.3± 7.4	-68.7± 7.7	0.13,0.27,0.37	2.08	24.6
129	N+ 0.3± 2.7	-68.8± 5.1	0.17,0.07,0.16	1.81	23.2
128	N+ 7.9± 0.2	-46.5±12.4	0.25,0.23,0.19	1.72	18.7
127	N+37.5± 5.8	-60.9± 1.1	0.28,0.34,0.23	1.47	16.4
126	N+61.8± 2.2	-77.3± 1.9	0.18,0.16,0.35	1.27	13.3
125	N+58.9± 6.5	-66.4± 5.2	0.14,0.11,0.16	1.72	15.5
124	N+64.1± 4.9	-63.1± 0.5	0.20,0.12,0.15	1.29	12.3
123	N+20.0± 7.3	-82.2± 7.3	0.13,0.19,0.19	1.73	17.5
122	S-85.7± 5.6	-66.6± 9.5	0.31,0.19,0.20	1.23	10.0
121	S+32.8±29.3	-57.9±12.2	0.16,0.14,0.20	2.65	15.7
120	N- 7.9± 9.9	-63.9± 4.3	0.10,0.10,0.13	2.90	16.5
119	S-10.0±19.6	-34.7± 2.2	0.30,0.15,0.19	1.52	14.0
118	S+19.0±17.2	-15.6± 2.0	0.43,0.30,0.13	0.85	10.1
117	S+ 8.5±22.2	-41.0± 2.4	0.56,0.19,0.35	0.81	8.8
116	S+27.5±17.8	-35.4± 4.0	0.18,0.21,0.16	3.03	25.6
115	S+24.9±13.4	-60.4± 4.0	0.15,0.22,0.24	2.53	19.1
114	S+19.8± 6.4	- 6.6± 2.4	0.30,0.31,0.11	2.06	21.0
113	S+20.6±17.9	-17.4± 3.9	0.25,0.17,0.11	1.64	16.2
112	S+12.1±12.1	+ 3.3± 5.0	0.56,0.12,0.08	1.46	14.6
111	S+ 7.2± 5.8	+ 8.3± 3.7	0.40,0.12,0.10	1.65	13.0
110	S+ 7.4±11.2	+ 0.1± 3.4	0.40,0.13,0.04	3.01	23.8
109	S+13.1± 1.2	+20.3± 2.8	0.24,0.09,0.05	2.70	14.6
108	S+18.2± 2.5	+27.5± 2.2	0.26,0.03,0.05	2.26	16.9
107	S- 0.2± 2.1	+22.4± 4.6	0.28,0.05,0.11	2.07	21.9
106	S+15.4±20.0	+ 5.9± 5.5	0.33,0.17,0.06	1.69	17.2
105	S- 0.5± 2.6	+29.2± 7.8	0.23,0.14,0.12	0.98	8.9
104	S+12.3±27.4	-15.3± 1.8	0.56,0.24,0.35	1.06	10.5
103	S+14.2±29.8	+ 1.6± 8.0	0.24,0.29,0.21	0.73	6.9
102	S- 4.3± 3.5	+35.0± 8.1	0.33,0.20,0.19	0.75	6.9
101	S+13.2±19.5	+ 7.2±28.4	0.29,0.18,0.29	1.07	9.2

The time required for the polarity transition was 4700 years, because it corresponds to the sedimentary record of 140 cm thick sediments (an interval between 240–100 cm below the key tuff). This value is in fairly good agreement with the period of 4600 years independently estimated by Cox *et al.* (1967) on the basis of statistical treatments of the polarity record in igneous rocks dated by the K-Ar method. The period of the geomagnetic intensity fluctuation, corresponding to the 200 cm thick sediments, is estimated to be 6700 years. This figure is a also almost consistent with the 8000 years period of intensity fluctuations estimated from the archeomagnetic data (Smith, 1967a,b, 1968).

Exact correlation of the world wide time plane will be possible with an error within about several hundreds years by tracing the positions of the virtual magnetic pole which drifted along the meridian during the reversal (Fig. 8). It will be also possible to trace the world wide time planes with an error less than 1000 years by the measurements of continuous samples taken from a stratigraphically controlled section to utilize the intensity fluctuations of the paleomagnetic field around the horizon of the reversal. If that the period of the intensity fluctuations of the paleomagnetic field was 7000–8000 years throughout geologic time is proved reliable, this may warrant the estimation of the rate of sedimentation from the measurement of the intensity fluctuations and the sedimentary thickness.

SEDIMENTOLOGICAL ANALYSIS

As previously mentioned, the sedimentological analysis was made on a quarter cut of the cored sample used for the paleomagnetic measurement. Altogether 72 samples

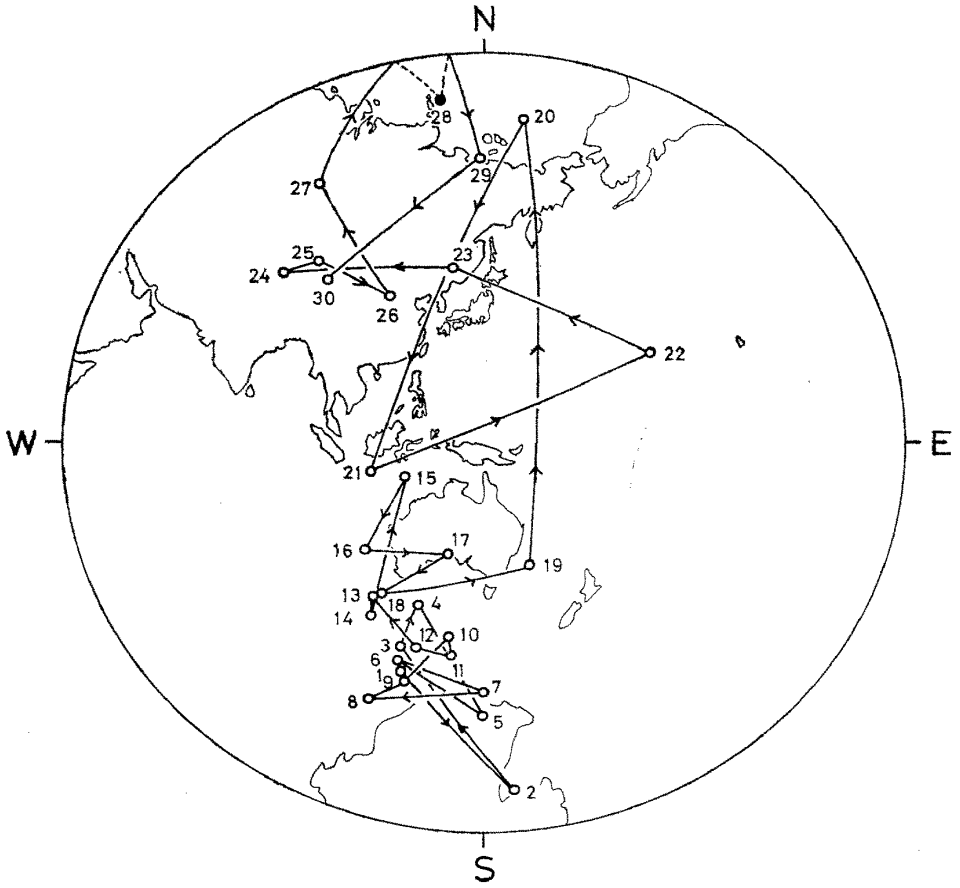

Fig. 8 Drift of virtual magnetic north pole during the reversal at the Matuyama-Brunhes boundary. The positions of the virtual pole are calculated from the data which are represented by points connected by line in Fig. 7.

have been analysed; their stratigraphic positions are shown in Fig. 5.

After soaked in water for one hour, the rock sample was disintegrated in water by a speed controlled mixer. The mud content (fraction of the grains finer than 4.0ϕ) and frequency curve for the fraction coarser than 5.0ϕ were obtained by the automatic grain-size analyser (Niitsuma, 1971).

The mud contents of the samples are rather uniform ranging from 70 to 85 percent, with two weak maxima at 65 cm and 260 cm below the key tuff (Fig. 9).

The grain-size distributions were found to be more or less similar in all samples, in that the fraction coarser than 3.0ϕ is small, and the fine fraction predominates. Sediments having a similar grain size distribution have been found in the studies of modern sediments along the Japanese coasts (Niitsuma and Mekata, 1971 a,b). They are found in areas where bottom conditions are judged to be calm hydrographically, although the depths of the water varies greatly. By analogy, the sediments from the horizons concerned in this study are interpreted to have been formed in a similarly calm condition. The comparison of the frequency curves obtained for each sample shows that they can be grouped into four types, representatives of which are shown in Fig. 10. The curves shown that the differences in composition exist in the fraction around 4ϕ in size; it appears that they are caused mainly by the removal of the grains around 4ϕ in size. It is considered that the sediments of type IV were the most affected by the removal while those of type I were uneffected.

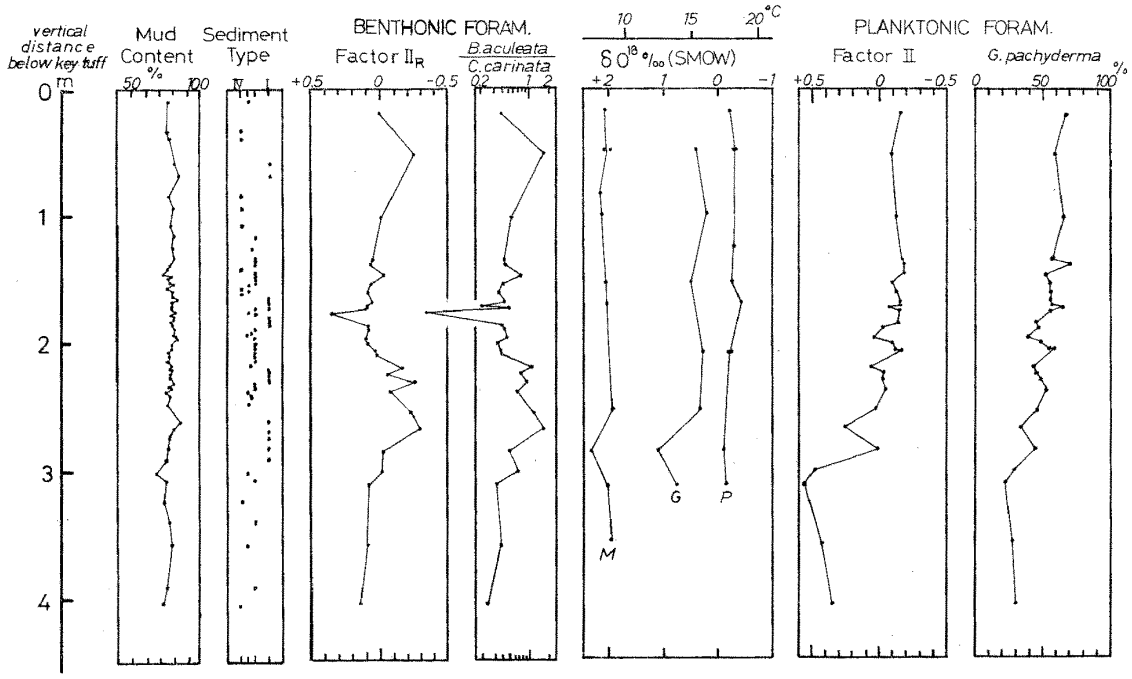

Fig. 9 Results of the grain-size analysis, paleotemperature measurement and the faunal analyses of Foraminifera. The samples dealt with are the same as those subjected to the paleomagnetic measurements (Fig. 4).

M: *Melonis barleeanus* G: *Globigerina pachyderma* P: *Pulleniatina obliquiloculata*

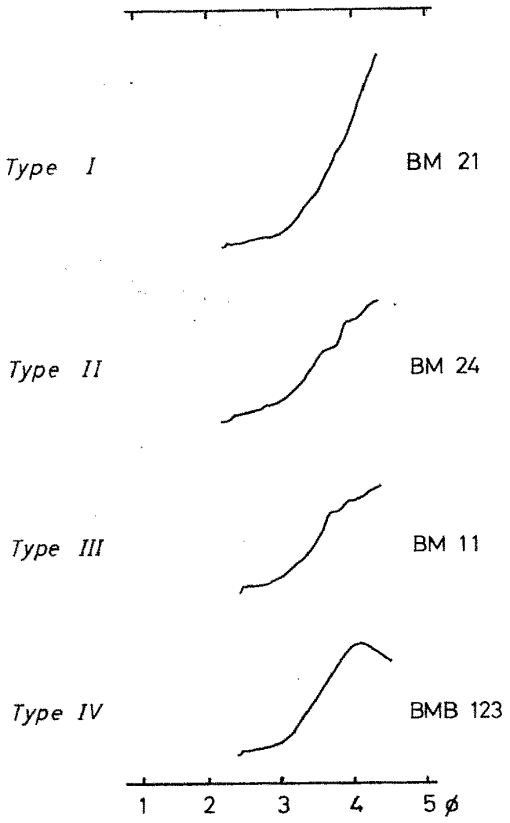

Fig. 10 Frequency curves of grain-sizes obtained by the automatic grain-size analyser. They represent four types.

In the present section the samples that fall in the type I are found from the horizons representing the five stratigraphic intervals as follow; 295 to 255, 213 to 210, 188 to 179, 173 to 163, and 80 to 50, all in cm below the key tuff (Fig. 9). These intervals which represent the calmest conditions are separated by other types of sediment. Although mud contents are rather uniform throughout the section, a tendency exists that they are higher in the above mentioned five intervals represented by type I. Of the five intervals, two, the uppermost and the lowermost correspond to the two maxima in mud contents. On the basis of these considerations it may be said that the water was deeper during the accummulation of the said two intervals than during the deposition of the rest of the section.

PALEOTEMPERATURE ANALYSIS

The purpose of the present study is to determine the changes in temperature of seawater as related to the reversal of the earth's magnetic field. The temperature of the sea water was determined by measuring the oxygen 18 content of the tests of Foraminifera which were abundant in the siltstones dealt with in the present study.

For the biogeneous calcium carbonate to be suitable for the purpose, the following requirements must be met. They are:

1) the biogeneous calcium carbonate must have been formed in the oxygen isotopic equilibrium with sea water,
2) the material must be contained in rocks in abundance so that one can gather a sufficient amount (ca. 20 mg) from the samples from every horizons taken at short stratigraphic intervals throughout the section studied,
3) the materials are tests of a single species throughout the section by which the influence due to the difference in the ecological behavior due to species can be eliminated,
4) the material is composed of sufficient numbers of monospecies specimens so that the individual difference in isotopic ratio can be averaged,
5) the ecological behavior of the species whose tests are used should be known, and
6) the oxygen isotope ratio of the tests must have remained unchanges since the biogeneous calcium carbonate was formed.

Among the many species of Foraminifera found in the section, the planktonic Foraminifera *Pulleniatina obliquiloculata*, *Globigerina pachyderma*, and the benthonic Foraminifera *Melonis barleeanus* were chosen for the oxygen isotope analysis.

The samples were collected at every 20 to 50 cm intervals vertically against the bedding plane between the key tuff and 4 m below it using a core sampler of 150 mm in diameter. The thickness of one sample was 5 cm and its weight was approximately 1000 g. After soaked in water for 24 hours, the rock sample was disintegrated in a speed controlled mixer. The sample was wet sieved through 42 and 80 meshes. The fraction between 42 and 80 meshes in size was dried and subjected to the separation into magnetic and nonmagnetic fraction by means of the Frantz isodynamic separater with the side tilt 30°, backward tilt 10°, and magnet charged with 1.0 A current. The magnetic fraction contains rock fragments and heavy mineral grains, whereas in the nonmagnetic fraction the remains of Foraminifera, Radiolaria, and the skeltons of other fossils are concentrated.

The tests of Foraminifera were picked up from the nonmagnetic fractions under a binocular microscope. Most of the chambers of the foraminiferal test were filled with authogenic pyrite. The foraminiferal tests of monospecies were pulverized with an agate motar and an ultrasonic generator. After drying, the fragments of the tests were separated from pyrite with the Frantz isodynamic separator (side tilt 30°, backward tilt 0.5°, and charged current of magnet 1.75 A).

The pulverized monospecies material was purified by roasting to destroy the organic substances in the sample powder. The apparatus used was the same as that described by Epstein *et al.* (1953), Horibe and Oba (1969), and Oba (1969) that roasts the material on Pt boats at 470°C with a stream of helium flowing at about 0.4 cc/sec. for 30 minutes. After this treatment the sample was reacted with pure H_3PO_4 to obtain CO_2 gass in a thermostat under the temperature precisely controlled at 25.00°C. The deviation δO^{18} ‰ of isotope ratio O^{18}/O^{16} in the CO_2 gass generated from each sample from that in the standard mean ocean water (SMOW) was measured by the Urey-Nier type mass spectrometer "PANDORA" (Horibe, 1966). The error in the oxygen isotope measurement mostly depends on the amount of the calcium carbonate sample; the error will be 0.028 ‰, when it weighs more than 12 mg, 0.079 ‰ when calcium carbonate is 5 mg, and 0.137 ‰ when it is 4 mg. Twelve milligrams of the sample represents approximately 1000 tests of *P. obliquiloculata*, 3000 tests of *G. pachyderma*, or 2000 tests of *M. barleeanus*.

Assuming that the oxygen isotopic composition of sea water in which the foraminiferal tests were formed was the same as that of SMOW, the paleotemperature can be determined from δO^{18} values of oxygen in the calcium carbonate tests by means of the scheme presented by Craig (1965).

The observed δO^{18} values (SMOW) ranged from –0.1 to –0.3 ‰ (from 17.3 to 18.1° C in paleotemperature) for the tests of *P. obliquiloculata*, from +0.2 to 1.1 ‰ (from 12.4 to 16.1°C) for *G. pachyderma*, and from +1.9 to +2.4 ‰ (from 7.2 to 9.2°C) for *M. barleeanus* (Table 4). The fact that these three species from the same sample gave quite different temperature from each other throughout the sequence appear to rule out the

Table 4 Paleotemperature measurements by Oxygen-isotope analysis.

Sample	species	$\delta^{18}O$‰(SMOW)	Sens of measurement ‰/div.
BM 38	P	– 0.21	0.785
	M	+ 2.07	1.368
BM 35	P	– 0.35	0.785
	P	– 0.32	0.785
	G	+ 0.41	0.993
	M	+ 2.10	0.785
	M	+ 1.97	0.785
BM 32	M	+ 2.17	1.368
BM 30	G	+ 0.20	0.993
	M	+ 2.15	0.785
BM 26	P	– 0.29	0.785
BM 23	P	– 0.25	0.785
	G	+ 0.49	0.993
	M	+ 2.06	1.368
BM 19	P	– 0.44	1.368
	M	+ 2.03	0.785
BM 15	P	– 0.20	0.276
	P	– 0.23	0.276
	G	+ 0.27	0.993
BM 10	G	+ 0.38	0.993
	M	+ 1.93	0.785
BM 05	P	– 0.12	0.785
	G	+ 1.11	0.993
	M	+ 2.35	0.785
BM 01	P	– 0.13	0.785
	G	+ 0.77	0.993
	M	+ 2.06	0.785
BM 40	M	+ 1.98	0.785

P: Pulleniatina obliquiloculata
G: Globigerina pachyderma
M: Melonis barleeanus

Table 5 Frequencies of benthonic Foraminifera.

BENTHONIC FORAMINIFERA \ LOCALITY	KM 93 1 A	KM 40 1 A	C1 1 B	C3 1 B	C5 1 B	C8 1 B	C10 1 B	C15 1 B	C20 1 B	C25 2 B	C30 1 B	C35 1 B	C38 1 B	EMB 101	103	105	106	110	112	113	115	116	119	120	121	123	125	127	130
Gaudryna sp.		1	2	2		1				1							2			1		1		1				
Goesella sp.				1			1				1												1	1	1	1		1	
Martinotticlla communis (d'Orbigny)	1		1			2	1	1		1		1			3	1				2	1	2	1	5	2	1	5	2	1
Sigmoilopsis schranbergeri Silvestri			1									1	1															
Nodosaria spp.				1		1		1							2		1						1			1		
Amphicoryna scalaris (Batsch)	2					1									3						1				1		1	
A. spp.		1						1				1				2			1		1		2		1	1		
Dentalina sp.						1					2																	
Lagena spp.					2			1	5										1	1		1	2		1	1		
Lenticulina lucida (Cushman)	1		1	3	2	1	2		2		2		1	1	1			2				1	3			4	1	4	1
Fissurina spp.	1		2	3	1		4	4			1	1	1	1	1	1	2	4	1	1	1	1		1			2	2	
Oolina spp.	2	3	1		2		2								1					1					1			1	1
Parafissurina spp.		1		3					2	2	3	1	2			1	4	2	7	2	2	1	1	2	3	2	2	1	1
Stilostomella spp.	1				2	1	1								2	2		1					2		2	1			2
Frondicularia sp.			1								2										1				1				
Buliminella elegantissima (d'Orbigny)	1		1	1	1	1	2			1						1		1	1	1	1		1		1			1	1
Bolivina pacifica Cushman and McCulloch								2										1		1						1	1		
B. robusta Brady	4	1						1		2				1	3	1			3		1	3	3		4	2		1	
B. subspinescens Cushman								1								1	2					1		1					
B. spp.	2		2			1	1	3		1	2	4			2	2	3	4	1	6		1	2	1			2	2	1	5
"B. " seminuda Cushman			1		2	1			1	2	1		1		1			1	1	1	1	1	1	1		2	1	2	1
Bolivinita quadrilatera (Schwager)	1				4	3	5	3	3			1		1	1			1	1	1	1					1		1	
Rectobolivina raphana (Parker and Jones)															1			1											
Bulimina aculeata d'Orbigny	5	7	10	16	14	29	23	9	3	8	14	25	9	15	33	14	27	9	9	10	11	9	1	12	10	11	8	21	7
B. marginata d'Orbigny	1										2										1		2	1					
B. pyrula spinescens Brady				1					1																				
B. striata d'Orbigny				1				1			1	1							1		1								
B. subornata Brady			1	1									1		1					1	1			1		1			
B. tenuata (Cushman)	1					1																					1		
Uvigerina proboscidea Schwager						1							1						1	1						1			1
Anglogerina anglosa (Williamson)	2		1	1	1	1		1			1			4	1	4	2	1	3	1	1	1		1	2	6	4	2	2
Trifalina bradyi Cushman								2	1												1		3		2		1		
Fursenkoina spp.		1								1															1				
Ehrenbergina sp.																				1									
Chilostomella ovoidea Reuss		1					1																						
Cassidulina carinata Silvestri	21	19	32	24	28	19	19	23	16	18	26	16	24	24	29	20	25	24	27	22	27	23	33	25	24	32	20	29	17
C. delicata Cushman	2	4	2	8	3	1	4	3	3	2	4	7	4	2			3	8			4		1	3	3	4	1	5	3
C. depressa Asano and Nakamura	8	11	8	12	10	5	10	7	11	14	18	12	4	3	10	7	16	7	15	11	8	14	19	9	6	13	14	20	3
C. kuwanoi Matoba	2	3	2	3	5	3		3	5	4	1	10	4	2	2	4	4	3	3	4	9	5	5	7	5	3	4	2	5	2
C. norcrossi Cushman				4									3																
C. orientalis Cushman	4	3	1	3	3	4	1	5	4	5	1	3		3	4	6	2	1	6	7	9	2	2	4	4	4		8	8
C. cf. oshimai Aoki					2																			1					
C. pacifica Cushman	4	6	11	11	2	8	6	6	6	7	2	8	4	6	14	10	5	6	13	9	8	6	15	18	9	13	14	12	16
C. parkerianus Brady	3	5		5	1	1	6	6	3	5	6	6	4	7	6	5	4	5	9	7	9	2		3	6	3	7	7	5
C. sagamiensis Asano and Nakamura	4			1	4	1										2			2				2		5	2			1
C. subglobosa Brady	4	1	6	2	6	1	3	2	6	5	2	5	4	3	3	3	2	3	5	3	5	6	5	4	5	4		2	2
C. sp. A			2			1	1	1		1	2		3	2			3	1	2	3		2						5	3
C. spp.		2	4	1	6			1	4		1	1	2	2		1	1												
Elphidium advenum (Cushman)	4	2	6	5	6	2	2		4	3		2	3	6	2		6	2		8	6	7	5	4	2	3		4	3
E. clavatum Cushman				1	1		1					1					1												2
E. crispum (Linné)		2				2	6	5					1	2	3		4	2	4				1	5	3	3	3	1	
E. kusiroense Asano	9	2	9	9	22	5	11	16	9	9	4	12	11	5	11	9	11	10	9	13	9	4	7	9	8	9	8	11	5
E. subarcticum Cushman	2	5	1	1		1	2	1				1		4	1	3		2		4	4		1		1	3	1		
E. subgranulosum Asano		1	2	2		1							3							2	1				1			1	
E. spp.	1		3				2		1						1			1							1				
Pseudononion japonicum Asano	7	4	5	7	1	3	8		4	2	2	4	2	3	4	4		9		5	4		1	2	4	4	4		
Astrononion umbilicatum Uchio		1				1		2						3	3				4	5	2	2				1	1	1	
Florilus labraduricum (Dawson)									2										1										
Nonionella pulchella Hada		1	1				1	1		2							1				2		1		1	2			
Pullenia bulloides (d'Orbigny)			2	1	1		1	6	3			2	4			2				2		2	3	1	2	1	3	2	
P. quinquelova (Reuss)			1			1			4							1													
P. salisburyi R. E. and K. C. Stewart								5		3	2		3		2			1	1		1				2	4		2	2
Melonis barleeanus (Williamson)	12	24	19	14	25	7	1	8	8	6	7	10	4	9	9	3	9	7	3	7	4	6	6	4	12	10	3	10	7
Cibicides aknerianus (d'Orbigny)	5	5	6	5	4	4	3	3	8	6	8	8	1	4	3	4	2	4	2	6	5	6	5		6	10	2	7	4
C. cf. aknerianus (d'Orbigny)	3	3		4		4		9				3			3	2		10		4	7	3	5	8		3		3	1
C. lobatulus (Walker and Jacob)	1						3		1		3	3		4	3					1		1			3				
C. cf. lobatulus (Walker and Jacob)	7	3		1	9	6	7	6	3	5	6	3	5		5	2	6		11	7	4	7	4	8	6	7	4	8	1
C. refulgens deMontfort	5	3	15	6	15	5	12	16	3	13	5	9	11	5	9	10	7	2	11	4	11	5	9	5	8	8	6	5	7
Hanzawaia nipponica Asano	5	3	1	9	5	3	2	6	5	5	7	5	10	5	4	3	7	4	1	8	4	5	7	11	8	5	7	8	4
Sphaeroidina bulloides d'Orbigny						1	1		1	1			1												1				
Buccella frigida (Cushman)	1			1		1	1		1					1		1								1			2		1
B. inusitata Andersen		1		1																							1		
Eoeponides sp.							1														1			2			2		
Epistominella naraensis (Kuwano)	36	38	51	41	55	44	43	34	50	40	53	28	59	60	29	52	65	44	50	29	35	52	27	38	33	49	41	52	38
E. nipponica Kuwano		1																									1		
E. sp. A				2		1										2				1			1		2		1		
E. pulchella Husezima and Maruhasi																													1
E. tamana (Kuwano)																													
Neoconorbina stachi (Asano)								1																			2		
Patellinella hanzawai Asano				1			1	1	1												1			1	1		1	1	
Rosalina bradyi (Cushman)	1			1				2	2		1	1								1				1					1
R. vilaredeboena d'Orbigny	3		2	3	1	2		2	1	3			2	3	4	3		9		3					4	1	7		1
R.? sp. A	5	3		1	3		2	1	2	4	2	5	1			2	1	3				1	3	1	2	1	1		4
Valvulineria nipponica Ishizaki																											2		
V. sadonica Asano					1																		2					1	2
V. sp. A	1					1													5	5	4	2	1	3			6	2	
Heronallenia stellata Takayanagi	1														2	1													
Pseudoeponides japonicus Uchio	11		9	9	25	10	15	24	13	9	6	9	4	10	15	8	1												
Ammonia cf. beccarii (Linné)	4			3	3	2	1	1	4	1	1	3	2		4		19	14	10	8	6	10	8	6	15	13	8	8	11
A. ketienziensis angulata (Kuwano)		4		4			1				1			1		3	1	1	1	1		2		1	1	2	2	2	2
A. sp. A		2	1		1	2	2								2	1	2		1	1	3		2					1	
Oridorsalis umbonatus (Reuss)	2		1	1	1	2	1	2				2												1	1	1		1	
Gyroidina orbicularis d'Orbigny	6	2	2	11		5	4	2	10	2	1	3	1	2	1	6	3	12	5	6	7	7	6	8	5	2	2	2	
"G. " nipponica Ishizaki			1	3		1	1	1	4	2		2	3		1					2	2			4	3	1	6	1	5
Hoeglundina elegans (d'Orbigny)			1		2	1					1			1	3				1		1			1	2		2	1	3
Total number	211	182	233	251	290	205	224	252	233	196	207	221	206	214	247	208	257	223	233	232	229	207	215	217	234	262	210	280	191

possibility of the exchange of the oxygen isotope ratio of the tests by diagenetic effects.

The δO^{18} value and paleotemperature at each stratigraphic horizon obtained for three foraminiferal species are shown in Fig. 9. No appreciable change is apparent from *P. obliquiloculata* and *M. barleeanus*. From *G. pachyderma*, however, the appreciable fluctuation of paleotemperature can be detected; it shows that the paleotemperature of sea-water in which *G. pachyderma* lived was 13.8°C at the horizon 313 cm below the key tuff, the lowest temperature 12.4°C at 286 cm below the key tuff and the paleotemperature rose to 15.4°C at the horizon 223 cm below the key tuff. Although the difference is small, it is of interest to point out that *M. barleeanus* showed almost a constant temperature of 9.2°C throughout the present section, has its minimum temperature (7.1°C) at the horizon 286 cm below the key tuff. At this horizon, 286 cm below the key tuff, *G. pachyderma* also showed lowest temperature (Fig. 9).

The constant difference of paleotemperature, ca. 10°C is found between the planktonic species, *P. obliquiloculata* and the benthonic species, *M. barleeanus*. It is considered that the difference of temperature was between the surface and bottom water column. Judging from the temperature gradient observed in the surface water column of the Pacific (Reid, 1965), the depth of water in which the sediments accumulated was estimated to be in the range of 200–300 meters.

CHANGE OF FORAMINIFERAL FAUNA

As mentioned previously the foraminiferal investigation was made on a quarter cut of the cored test piece used for the paleomagnetic measurements. The 29 samples were collected from the 4 m thick interval below the key tuff at stratigraphic intervals ranging from 3.5 to 50 cm (Fig. 5). After soaked in water for one hour, the rock sample was disintegrated in a water bath. After 15 minutes run in a controlled mixer at its slowest speed, the sample was wet sieved through 200 mesh and dried. The tests of Foraminifera were concentrated by making use of the Frantz isodynamic separator (side tilt 30°C, backward tilt 10°C, and magnet charged with 1.0 A current) and were picked up under a binocular microscope. In the present article, the faunal change of Foraminifera is analysed by the principal factor analysis (Harman, 1967; Imbrie *et al.*, 1962) and in terms of Motomura's Plane (Niitsuma, 1968). All calculations have been done with the electronic computer (NEAC 2200, Model 500) in the Computer Center of the Tohoku University (Niitsuma *et al.*, 1971).

1) Faunal change of benthonic Foraminifera

In the present study, only the tests of Foraminifera coarser than 74 microns have been identified. At least 200 benthonic specimens have been identified for each sample, resulting in recording altogether 95 species in 50 genera from the samples. In the samples studied the species that occur in abundance are: *Epistominella naraensis* (Kuwano), *Cassidulina carinata* Silvestri, *Melonis barleeanus* (Williamson), *Bulimina aculeata* d'Orbigny, *Pseudoeponides japonicus* Uchio, *Cassidulina depressa* Asano and Nakamura, *Elphidium kusiroense* Asano. Their abundance point to the faunal characteristics of the zone 6 defined by Aoki (1963) in the Yoro Valley section (Table 5).

On the basis of relative frequencies of 70 species, factor analysis has been made to determine the relationship between benthonic foraminiferal faunas of 29 samples (Table 6). All loadings of the first factor are found positive and the loadings express the common component in faunas of all samples. The loadings of the other factors express the different component. The total loading of the first factor in all faunas is 91.0%, that of the second factor is 2.2% and that of the third factor is 1.85%. However, the first factor express the

Table 6 Data of Factor analysis of benthonic foraminiferal faunas.

Sample	FACTOR 1	FACTOR 2	FACTOR 3	FACTOR 4	FACTOR 5	FACTOR 6
KM 93	.95363	.10031	-.09732	-.15799	-.02521	-.02630
BM 40	.88757	.14182	.02038	-.11276	-.34265	-.02517
01	.95634	.08383	-.02219	-.11818	-.08321	-.00185
03	.96326	-.04614	-.02242	-.03131	-.11955	-.14277
05	.97992	-.01552	.01896	-.29683	.01961	.11444
08	.93121	-.22089	.21394	.05854	-.03865	-.06637
10	.93913	-.19014	.14838	.01317	.11949	.05164
15	.89093	-.09247	-.11584	-.19669	.27953	.00649
20	.93095	.22173	.09578	-.06054	.05675	-.01592
25	.97025	.06620	-.01831	.01181	.04207	.13699
30	.95743	.08314	.11558	.07684	-.10308	.12249
35	.93112	-.34796	.01866	-.03446	-.13202	.04062
38	.94669	.15651	.15071	.04358	.05817	.01036
BMB 101	.95698	.09388	.21096	.00165	-.00804	-.07017
103	.86597	-.44896	-.05418	.01387	-.02185	.01428
105	.96812	.04682	.13061	.08565	.07926	-.05553
106	.96522	-.06729	.18835	.00564	.01781	.07578
110	.93596	.05811	.01231	-.07264	.06563	-.21329
112	.95504	.07973	-.03760	.13594	.09911	.10746
113	.92657	-.06276	-.19433	.06387	-.03578	-.02240
115	.94916	-.02795	-.13911	.08255	.02796	-.08309
116	.96822	.14448	.05946	.06760	-.01633	.08813
119	.85735	.08592	-.42746	.06760	-.04112	.07573
120	.93997	-.02309	-.14623	.19090	.02246	-.11501
121	.95316	-.02740	-.09718	-.14475	.04610	-.00662
123	.98192	.04862	-.07023	-.00779	-.01618	.03710
125	.94023	.07411	-.00539	.16844	.05362	.02979
127	.97365	-.05349	.00174	.11033	-.09292	.04576
130	.94490	.07795	.00842	.01514	.07500	-.11218
eigen value	25.5804	.6170	.5192	.3454	.3153	.1998
total load of each factor in %	91.00	2.20	1.85	1.24	1.12	.71

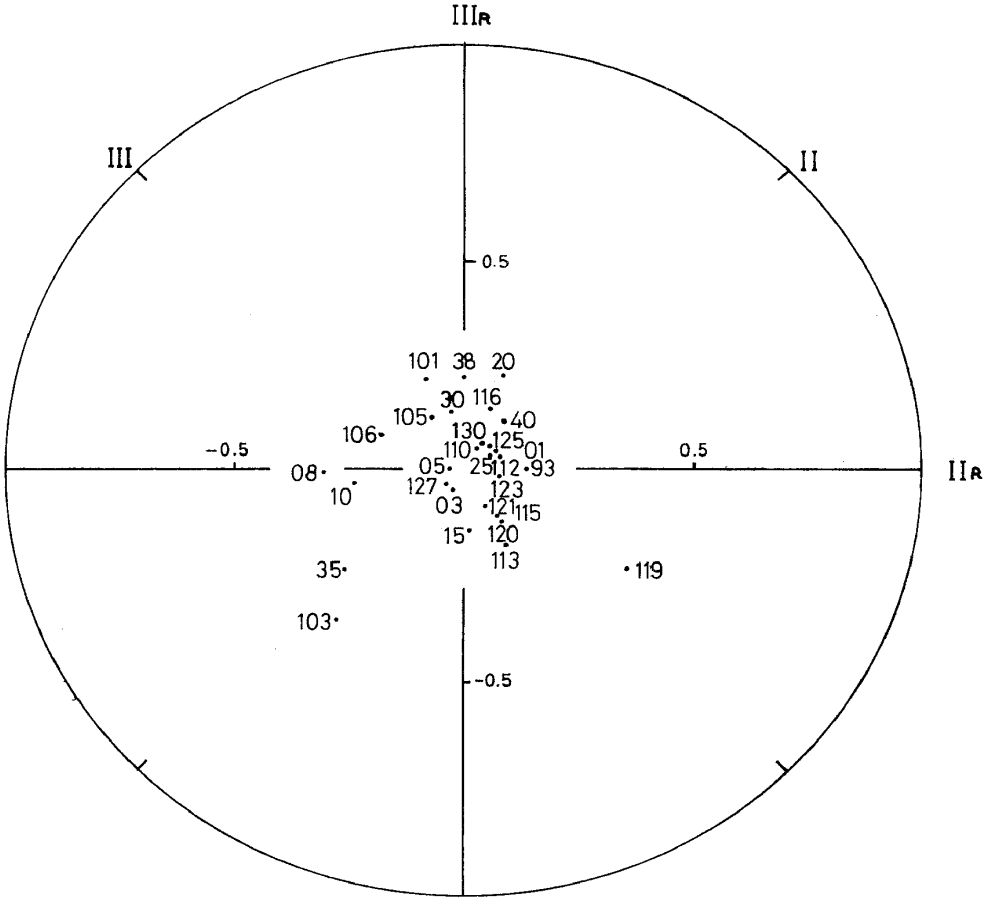

Fig. 11 Benthonic foraminiferal faunas plotted with respect to Factor axes II_R and III_R. The numbers are sample numbers.

common component in faunal change of all samples and the second and third factors express 44.4% of the different component in faunal change. In Fig. 11, and faunas of 29 samples are plotted in coordinates projection by mean of the loadings of the second and the third factors. Because the axes of factors by factor analysis are decided by mathematic computation, the direction of the axes do not always fit for interpretation of the faunal changes. To make the interpretation of the faunal change easy, the axes of the second and third factors were rotated 45° dextrally from their original positions II and III to II_R and III_R in this projection. In figure 11, the loadings of factor II_R represent the whole change of the fauna through the stratigraphic horizon and the value differs less when the stratigraphical horizons are closer. The change of the loadings of II_R with stratigraphic horizon is shown in a column of Fig. 9. From Fig. 9, it is obvious that the value of II_R is reflected well by the ratio of *C. carinata* to *B. aculeata*. It appears that the majority of the benthonic foraminiferal change can be explained by the ratio of *C. carinata* to *B. aculeata*. According to Aoki (1968), *C. carinata* lived on bottoms shallower than *B. aculeata*. Therefore, the ratio is considered to be a measure to estimate the depth of water in a relative manner.

The ratio *B. aculeata* / *C. carinata* shows the maxima at 260 cm and 50 cm below the key tuff and accordingly II_R shows the minimal values at these horizons. Hence, it is infered from the benthonic Foraminifera that water was deepest at these two horizons. The two horizons are close in position to 270 and 65 cm, respectively which represented the highest values of mud contents and only type I sediments, have been judged to be of the

deepest water from the grain-size analysis.

At the horizon in which the ratios show the shallower depths, the sediments tend to have lower mud content and are usually represented by type II and/or III (Fig. 9). This is interpreted to have resulted from the removal of 4ϕ grains from the type I, that took place only in shallower depths.

The change in the benthonic foraminiferal fauna occurred in cycles of about 200 cm period and agrees with the change of the sediments. The length of the period also agrees with the period in the change of geomagnetic intensity. At the horizon of the earth's magnetic field reversal no apparent change in benthonic foraminiferal fauna was recognized.

2) Faunal change of planktonic Foraminifera

In the present study, only the tests, coarser than 125 microns have been identified. At least 200 planktonic specimens have been identified for each sample, resulting in recording altogether 24 species in 9 genera. In the 29 samples studied, the following species are abundant: *Globigerina pachyderma* (Ehrenberg), *G. falconensis* Blow, *Globigerinoides ruber* (d'Orbigny), *Globoratalia inflata* (d'Orbigny), *Globigerinita glutinata* Egger, *Globigerina immaturus* LeRoy (Table 7).

Factor analysis has been applied to analyse the changes that took place in the planktonic population during the time represented by this section. The analysis is made on the bases of the relative frequencies of 24 species in each of the 29 samples (Table 8). Only the largest three factors, Factor 1, 2, and 3, are considered in the following discussion. It was found that the first factor remained virtually unchanged throughout the section, and the total of its loadings is 93.6% of that of the all factors, indicating that the species composition and their proportion did not change greatly during the time-interval. The total loadings of the second factor is 4.5% of that of the all factors, that of the third factor 0.5%. Since the first factor is virtually constant, the changes observed in the second factor is important, particularly in view of that the second factor expressed the most (70.5%) of the loadings after the first factor has been excluded (Fig. 12). The loadings of the second factor changes greatly in the horizons (Fig. 9). The comparison of the curve with that in the next column (given for the proportion of *G. pachyderma* in the planktonic foraminiferal assemblage) suggests that *G. pachyderma* accounts decisively for the changes. It is revealed, therefore, that the proportion of *G. pachyderma* represents, in effect, the larger part of the difference in the planktonic foraminiferal faunas through the stratigraphic interval.

As shown in Fig. 9, *G. pachyderma* takes about 30% of the planktonic population in their horizons lower than 300 cm below the key tuff; the proportion increases upward to more than 65% at 139 cm after fluctuating at intermediate horizons, e.g. 45% at 285 cm, 39% at 278 cm, all below the key tuff. After attaining 65% at 139 cm below the key tuff, the proportion remains above 60% through the rest of the section up to the key tuff. In this change, the first increase in frequency of *G. pachyderma* at the horizon 285 cm below the key tuff corresponds to the temporal lowering of the paleotemperatures measured for the tests of *G. pachyderma* and *M. barleeanus* (Fig. 9). In the rest of the sequence up to the key tuff, however, the change of paleotemperature does not correspond to the fluctuations shown in the frequencies of *G. pachyderma*.

Fig. 13 shows another result from the factor analysis. It is to determine the species to species relationships that were maintaind by planktonic Foraminifera during the accummulation of the present section. In Fig. 13 all planktonic species are plotted in coordinates projection by means of the loadings of the first and second factors. In this projection the point representing *G. pachyderma* is found isolated from the points of the other species, indicating that the frequency of *G. pachyderma* changes in horizon independ-

Table 7 Frequencies of palnktonic Foraminifera.

PLANKTONIC FORAMINIFERA \ LOCALITY	KM 93 1 A	BM 40 1 A	01 1 B	03 1 B	05 1 B	08 1 B	10 1 B	15 1 B	20 1 B	25 2 B	30 1 B	35 1 B	38 1 B	BMB 101	103	105	106	110	112	113	115	116	119	120	121	123	125	127	130
Globigerna bulloides d'Orbigny									1																				
G. calida Parker			5	2	1			1	1	4		3	2			3	3	4		4	4	3	2	1	6	2	2	3	5
G. cf. calida Parker	3	3																		2									
G. falconensis Blow	44	42	37	52	24	42	20	44	12	17	17	26	16	23	34	20	29	8	17	24	22	12	16	20	12	16	21	9	12
G. imcompta Cifelli	7	8	5	6	4	11	3	32	1	4	4	5	4	4	34	11	11	8	17	16	12	23	22	2	13	15	14	24	19
G. pachyderma (Ehrenberg)	65	55	37	57	97	83	71	289	129	167	120	153	122	116	129	94	86	109	114	84	104	103	138	106	105	124	116	108	115
G. quinqueloba Natland	17	10	2	7	3	7	5	3	1	4	4	4	1	6	1	3	1	9	1	4	1	9	5		3	2	3	4	3
G. rubescens Hofker	12	14	10	9	23	7	6	27	11	7	4	12	7	4	14	11	8	14	5	16	11	10	5	18	4	5	8	9	13
Globigerinella siphonifera (d'Orbigny)																			1										
Globigerinita glutinata Egger	20	18	8	14	22	17	7	20	12	15	9	7	5	14	14	27	18	22	23	21	20	17	17	15	21	26	15	13	15
G. uvla (Ehrenberg)			1						1					1								5							
Globigerinoides conglobatus (Brady)		1															1			1									
G. immaturus LeRoy	6	3	2	3	1	7	6	9		2	1	3	2	2	5		3		2	4	1	1	2	1	2			4	
G. ruber (d'Orbigny)	19	19	20	13	12	22	12	28	13	4	11	15	9	23	13	17	15	9	21	28	21	19	14	11	11	12	9	10	9
Globoquadrina dutertrie (d'Orbigny)	11	2	10	2		9	3		1	1	1	13			2	5		8		5	6		5	10			3	6	
Globorotalia crassaformis (Galloway and Wissler)	6	4	5	3	3	5	5	5	1	4	3	7	8	3		3	3	3	2	2	2	3	7	6	6	5	6	5	
G. crassula Cushman and Stewart	8	5	3	3	3		3	6	4	3	4	3	2	2	4	6	4	4	6	3	6	4			1		3	3	3
G. inflata (d'Orbigny)	8	12	11	17	9	21	8	15	9	2	5	6	2	4	12	5	11	3	5	5	17	3	8	6	3	5	6	7	6
G. menardii (d'Orbigny)	1			1	2			3			2					1			1	1				1	2	1	1	1
G. tosaensis Takayanagi and Saito												1	2											1					1
G. tumida (Brady)			2												1	1	1		1					1	1	1			
Orbulina universa d'Orbigny					1						1											1			1			1	
Pulleniatina obliqueloculata (Parker and Jones)	7	14	11	11	13	14	6	9		2		6	1	1	2	3		5	12	3	2	4	1		1	8	3	3	2
Sphaeroidinella dehiscens (Parker and Jones)								1										1							1				
Total number	231	210	172	203	218	245	155	492	197	236	186	261	183	221	268	210	202	199	232	223	225	231	246	194	192	223	210	210	204
Benthonic Foraminifera %	20	19	25	29	30	36	29	21	22	17	19	26	18	21	28	18	26	22	14	21	22	24	18	22	26	26	27	26	23

Table 8 Data of Factor analysis of planktonic foraminiferal faunas.

Sample	FACTOR 1	FACTOR 2	FACTOR 3	FACTOR 4	FACTOR 5	FACTOR 6
KK 93	.90841	.37207	-.01876	.05225	-.00550	-.16754
BM 40	.88437	.44929	-.04197	.08120	-.04743	.00207
01	.79722	.57650	.02179	-.08063	.12122	.07088
03	.85217	.49926	.07199	-.00698	-.12475	.01304
05	.98168	.02629	.01046	.14765	-.02464	.08669
08	.95253	.27293	.00985	-.06551	-.01120	.00615
10	.99074	.04455	.09747	-.01290	.02379	-.02482
15	.99054	-.10861	.04048	-.03608	-.01628	.03003
20	.98275	-.14717	.08014	.03251	.03869	.02775
25	.97856	-.17190	.09980	.01817	-.02088	-.02338
30	.98680	-.12148	.09169	-.00790	.01192	-.02991
35	.99601	-.08666	.11529	-.03779	.04662	-.01363
38	.98125	-.14171	.11769	-.01657	.01754	-.00427
BMB 101	.99156	-.04046	.03998	.00584	.07796	-.05127
103	.98239	-.01579	-.06091	-.12556	-.09152	.03506
105	.98870	-.02395	-.09767	.09089	.00663	-.00010
106	.99056	.07963	-.02267	-.03775	.00296	-.00079
110	.97830	-.16595	-.02330	.10614	-.01575	-.01511
112	.98778	-.07653	-.07944	-.00709	.02979	-.00367
113	.97692	.06783	-.15693	.01326	.10436	.01390
115	.99142	-.01017	-.04206	.00801	.01917	.06379
116	.97993	-.12681	-.12179	-.04045	.01817	-.03659
119	.98497	-.14117	-.02124	-.07850	-.00681	-.03220
120	.98848	-.06168	.06470	.07533	.01714	.05306
121	.98394	-.14945	-.04065	.01415	-.01441	-.02561
123	.98715	-.12038	-.04058	.02646	-.03358	-.00280
125	.99421	-.08750	.01795	-.02359	-.03877	-.00686
127	.97617	-.17579	-.06492	-.08540	-.03779	.00174
130	.98350	-.15714	-.04023	-.01511	-.04641	.03706
eigen value	27.1709	1.2912	.1486	.1061	.0726	.0604
total load of each factor in %	93.63	4.45	.51	.36	.25	.21

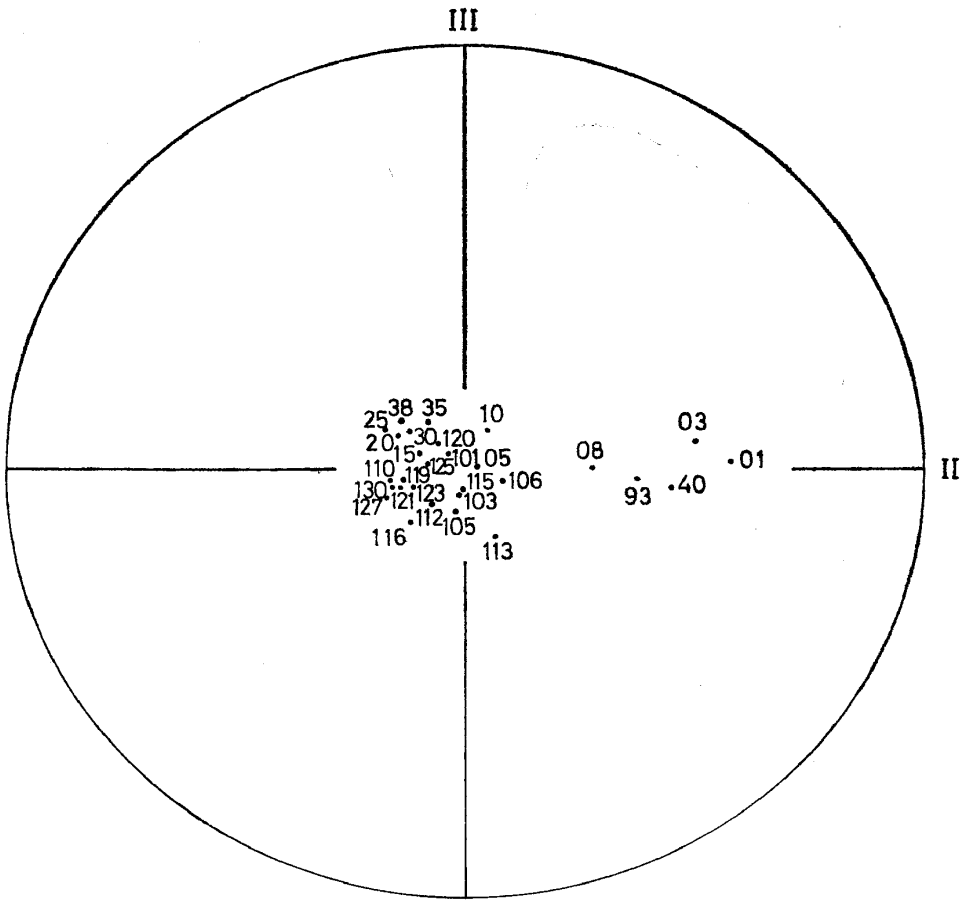

Fig. 12 Planktonic foraminiferal faunas plotted with respect to Factor axes II and III. The numbers are sample numbers.

ently with other species.

Fig. 14 shows the result of plotting on the Motomura's Plane (Niitsuma, 1968), in which a vertical axis is "a" and a horizontal axis is "B" of the values computed by the equation:

$$\log y + a(x-1) = \log B \tag{1}$$

where x is the rank of frequency of a species in the fauna, 6 is the frequency of species in percent, a and B are constants calculated by the least square method using the frequencies of six higher ranked species in the fauna. Because the frequency of species, y is expressed in percentage, the sum of y of all species in a fauna would be 100. Thus the relation,

$$B = 100\left(1 - \frac{1}{10^a}\right) \tag{2}$$

is lead from the equation (1) that gives a curve (Motomura's Line) in Fig. 14. Whether a given fauna fulfills the relation suggested by Motomura (1932) can be determined by the values of a and B obtained for the fauna by the equation (1). If a fauna statisfies the relation of logarithmic normal distribution or a fauna is a mixture of faunas which satisfy the relation of equation (1) (Preston, 1948; Nobuhara *et al.*, 1954; Whittaker, 1965), the point for the fauna would be located on the upper leftside of Motomura's Line (Niitsuma, 1968; Niitsuma *et al.*, 1971). Ujiié (1968) reported that the living planktonic Foraminifera in the Indian Ocean satisfied Motomura's relation, though he misused, the term of the

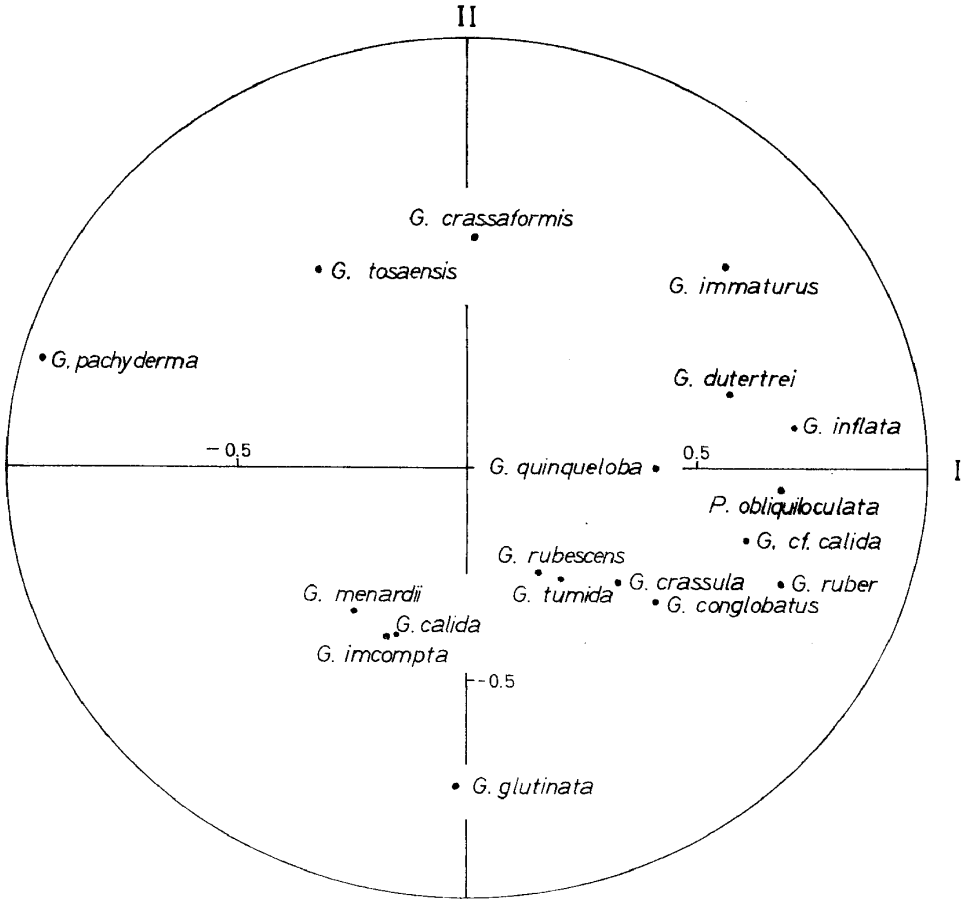

Fig. 13 Planktonic foraminiferal species plotted with respect to Factor axes I and II.

logarithmic normal distribution for this relation. The points obtained for the planktonic foraminiferal faunas treated in this study, however, do not fall near Motomura's Line but scatter widely in the upper region (Fig. 14). When the plots are made excluding *G. pachyderma* from the faunas points are well alined along Motomura's Line (Fig. 15). However the results are interpreted as suggesting that *G. pachyderma* belonged to a different ecosystem from that of other planktonic foraminiferal species. This interpretation is born out by the other data: 1) the proportion of *G. pachyderna* changes in horizon independently with other species (Fig 13); 2) paleotemperatures derived from the tests of *G. pachyderma* differ largely and show different change from that of *P. obliquiloculata* (Fig. 9). The interpretation seems to be quite reasonable also in view of the modern geographical distribution of these two species: according to Bradshow (1959), *G. pachyderma* is a representative of the cold water mass; *P. obliquiloculata* is of the warm water mass to which group the other species occuring in the present section belong.

The mixture of cold and warm water species in a thanatocoenosis from every rock sample can be explained by the migration at the time of the boundary between cold and warm currents in the depositional envirnoment. It is maintained here that the composition of the thanatocoenosis in the present section depended upon the duration of the current that dominated the area, rather than the fluctuation of faunal composition through time that took place within a single water mass. It appeared that a slight change in water temperature took place in *G. pachyderma* carrying cold water at 285 cm below the key tuff, and after that the temperature remained virtually constant. The general trend of increase of the

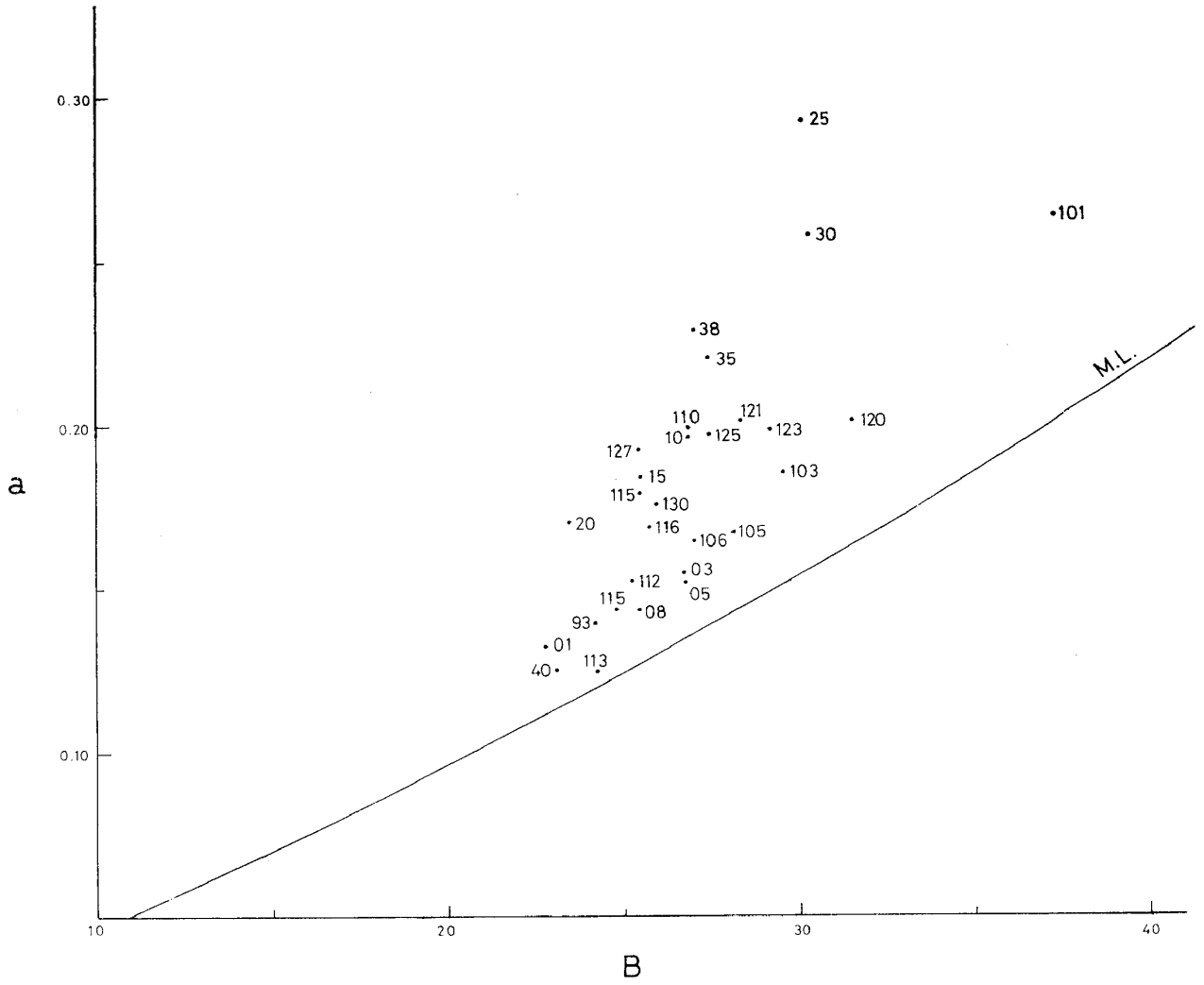

Fig. 14 Plots of a and B obtained for 29 planktonic foraminiferal faunas on the "Motomura's Plane".

proportion of *G. pachyderma* commenced from 255 cm level is the reflection of the change that cold water current occupied the area for a longer time than before. The increasing frequency of *G. pachyderma* is found between 255 and 139 cm below the key tuff and this period is coincident with that of the geomagnetic reversal between 240 and 100 cm below the key tuff.

CONCLUSION

The behavior of the earth's magnetic field during reversing at the boundary between the Matuyama and Brunhes Polarity epochs has been revealed in detail by measuring DRM of the sedimentary sequence accummulated with high rate of sedimentation. The results show that the time of duration in which the field completed change of its polarity was approximately 4700 years. Intensity of the magnetic field fluctuated with a period of approximately 6700 years around the reversal and attained its minimum value at a reversing time. During the polarity change the position of the virtual magnetic pole drifted along the meridian of 120° E.

The depth of water under which the sediments accummulated appears to have remained within 200–300 m; the depth estimate is based on the finding that the

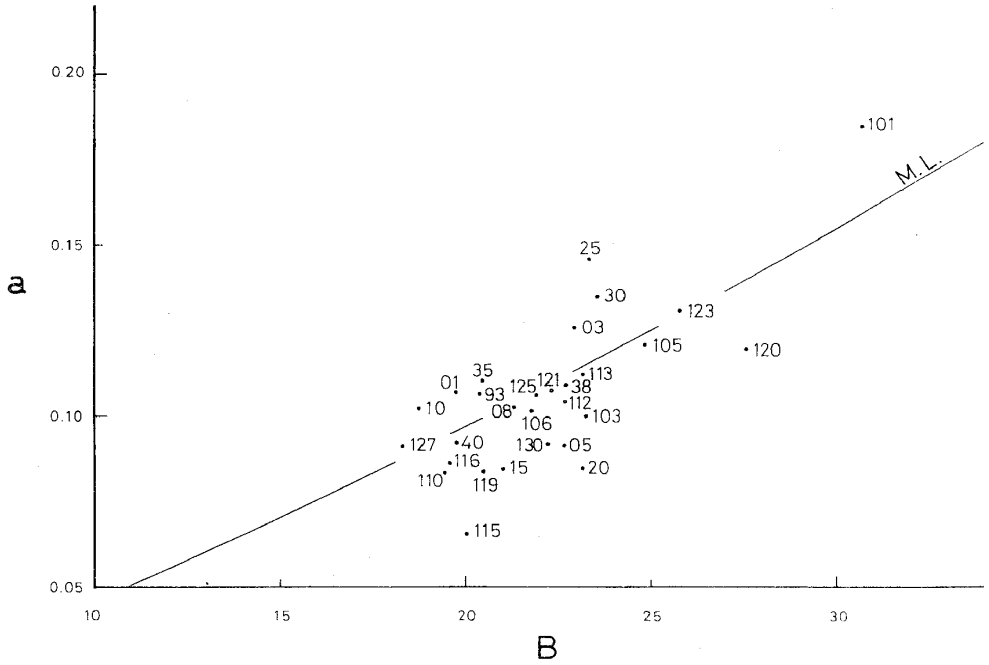

Fig. 15 Plots of a and B obtained for 29 planktonic foraminiferal faunas without *Globigerina pachyderma* on "Motomura's Plane".

paleotemperature differed by 10°C between the surface and the bottom of the water-column during the deposition. Within this rather narrow range, the depth of water fluctuated with a period of approximately 7000 years; its phase, however, does not appear to have been related particularly to the magnetic field reversal. The change in water temperature in *P. obliquiloculata* carried by a warm current is judged not to have been appreciable, on the basis of the isotopic measurements on the tests of this species. No appreciable change has been detected for the cold water current which also occupied the area during the accummulation of the sedimentary sequence, except a decrease by 3°C detected at one horizon from the isotopic measurements of the tests of a planktonic species *G. pachyderma*. This horizon of a temporal cooling has also been detected by the benthonic species *M. barleeanus*, also measured isotopically, and is estimated to have taken place approximately 1000 years before the field reversal commenced. Whether this cooling was related causually to the magnetic reversal is still open to question.

Change simultaneous with the magnetic field reversal has been found in the relative frequencies of planktonic Foraminifera. It is particularly represented by a cold water planktonic species, *G. pachyderma*, whose proportion increased gradually from 30% before the reversal to as much as 60% after the completion of the reversing, while the temperature of water remained virtually unaltered. The increase in proportion is, therefore, interpreted to reflect a longer stay of the cold water-masses in the locality during and after the reversal than before.

Finally various lines of evidence indicate that the magnetic field reversal at the boundary of Matuyama-Brunhes Polarity epochs can be related to the change in the circulation pattern of superficial water-masses that caused an influx of cold water into this area in the northwestern Pacific compared with the period before the geomagnetic polarity change.

Table 9 Data of Factor analysis of planktonic species.

species	FACTOR 1	FACTOR 2	FACTOR 3	FACTOR 4	FACTOR 5	FACTOR 6
Globigerina bulloides	.21047	.47648	-.28544	-.03583	-.10679	.25449
G. calida	-.15186	-.39621	.58987	-.13708	-.27415	.25846
G. falconensis	.85660	.14589	.04183	-.12626	.22136	.01177
G. pachyderma	-.91940	.25399	.00593	.12693	.03561	-.08642
G. quinqueloba	.41364	.00164	-.52674	-.22709	-.21839	.13829
G. rubescens	.15911	-.24882	.09901	.11059	.52907	.03038
Globigerinita glutinata	-.02955	-.75174	-.11247	-.15785	.17118	.23278
G. uvla	.02419	-.17895	.01328	-.04991	-.57442	-.50319
Globigerinoides conglobatus	.41372	-.31057	.06967	.53441	.05866	.28851
G. immaturus	.56217	.47061	-.29919	.11647	-.25624	.34734
G. ruber	.68362	-.27081	.08301	.24286	-.20165	-.02618
Globoquadrina dutertrie	.57149	.17600	.14882	.10402	-.53345	-.00579
Globorotalia crassaformis	.01845	.54253	.30225	-.35069	-.16952	.45445
G. crassula	.32848	-.26737	-.30882	-.00847	.09794	-.28018
G. inflata	.71287	.09338	.02738	-.10452	.22951	-.17166
G. menardii	-.24361	-.35575	-.41730	-.24169	.26586	.18421
G. tosaensis	-.32519	.46475	.44414	.16358	.22338	.06468
G. tumida	.20555	-.26072	.66155	-.29884	-.07306	.04176
Pulleniatina obliquiloculata	.68510	-.05003	-.10732	-.40314	.19351	.03429
Orbulina universa	-.30065	-.26224	-.29546	-.38117	-.30956	.05057
Sphaeroidinella dehiscens	-.31805	-.28187	.02792	-.39807	-.11802	.50323
Globigerina cf. calida	.61015	-.16618	.46436	-.21291	.06341	-.17505
Globigerinella siphonifera	.15255	-.34132	-.02039	.68919	-.06737	.44245
Globigerina imcompta	-.16750	-.39495	-.07062	.16910	-.47631	-.08456
eigen value	5.0337	2.7870	2.1718	1.8359	1.8176	1.5161
total load of each factor in %	20.95	11.62	9.04	7.64	7.56	6.31

APPENDIX

PROGRAM OF ELECTONIC COMPUTER FOR DATA OF PALEOMAGNETIC MEASUREMENT

Numerical analyses of data obtained from the present paleomagnetic measurements were processed through a high speed numerical calculation by the Electronic Computer, NEAC 2200–Model 500 at the Computer Center of Tohoku University. In this Appendix, the processes of the analysis and program for electronic computer are described.

A series of values had been obtained by measurement at every 30° around three orthogonal spin axes of one sample. From them the error caused by linear drift of the magnetometer was corrected by using the values of the first and last measurement, A_1^m and A_{13}^m, in a spin for the fixed axis.

$$Ai = \frac{(A_1^m - A_{13}^m)(i-1)}{12} + Ai^m$$

where, Ai is the value after this correction, and Ai^m is i-th measured value in a spin.

The measured value is generally distributed along a sine curve when it was plotted. Two orthogonal components, Va and Vb, of the projection of the magnetic moment upon a plane normal to the spin axis are calculated through Fourier analysis:

$$Va = \frac{2}{12} \sum_{i=1}^{12} Ai \cos\{30° \times (i-1)\}$$

$$Vb = \frac{2}{12} \sum_{i=1}^{12} Ai \sin\{30° \times (i-1)\}$$

The standard deviation, SD, is determined as a ratio of mean distance of the plotted intensities Ai versus a sine curve calculated from measured values:

$$SD = \frac{\sqrt{\frac{1}{12}[Va \cos\{30°(i-1)\} + Vb \sin\{30°(i-1)\} - Ai + \overline{Ai}]^2}}{\sqrt{Va^2 + Vb^2}}$$

where, $\overline{Ai}$ is average value of the measured value of a spin, $A_1 \ldots . A_{12}$, and $\sqrt{Va^2 + Vb^2}$ is an amplitude of the sine curve.

Three pairs of orthogonal components of magnetic moment and three standard deviations of each spin are calculated, and from those values the weighted average of three orthogonal components of magnetic moment by the standard deviation are calculated by the equation:

$$V = \frac{SD_2 V_1 + SD_1 V_2}{SD_1 + SD_2}$$

where, V is the averaged value; SD_1 and SD_2 are the standard deviations, respectively of measurements from which V_1 and V_2 are calculated.

The three orthogonal components of magnetic moment of a sample are translated into the components, V_{NS}, V_{EW} and V_{UD}, at the present sampling position and these at the time when the sediments had accumulated, by rotation of the coordinated, taking into the account of the directions of the sample and of the bedding plane. Declination D, and inclination I, of magnetic moment are calculated from the components:

$$\tan I = \frac{V_{UD}}{\sqrt{V_{EW}^2 + V_{NS}^2}}$$

$$\tan D = \frac{V_{EW}}{V_{NS}}$$

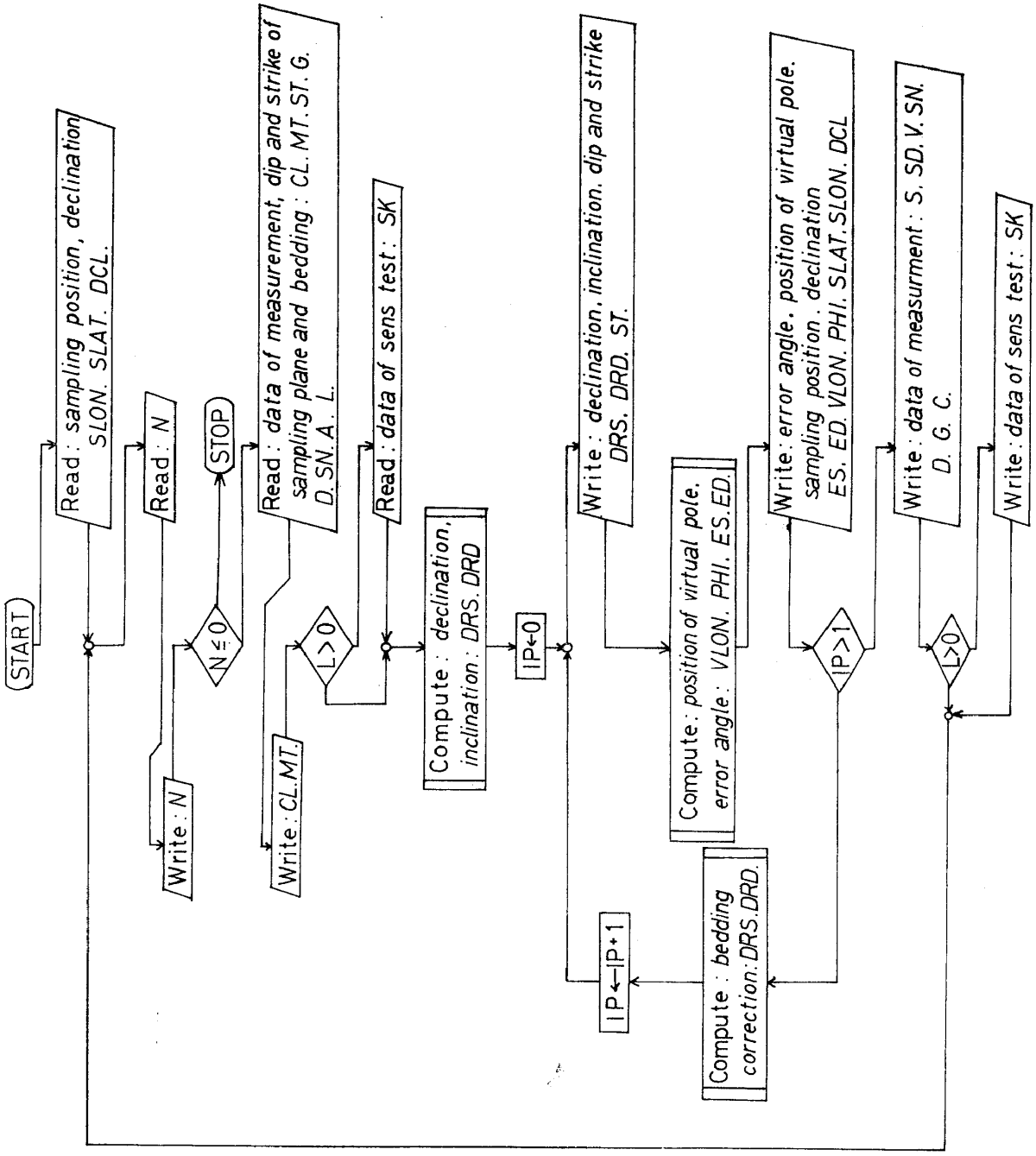

Fig. 16 Flow chart of the program for analysis of paleomagnetic data.

```
C       ANALYSIS OF PALEOMAGNETIC DATA
        DIMENSION D(3),ST(2,2),MT(2),SN(3),A(13,3),SK(14),V(5,3)
        DIMENSION VA(3),VB(3),SD(5),C(13,3)
        READ(11,87) SLON,SLAT,DCL
     87 FORMAT(3F5.1)
      1 READ(11,80) N
     80 FORMAT(I5)
        IF(N) 2,2,3
      3 READ(11,81) CL,(MT(I),I#1,2),((ST(I,J),I#1,2),J#1,2),G
     81 FORMAT(A8,I12,I10,4F5.1,F6.1)
        READ(11,82) (D(J),J#1,3),(SN(J),J#1,3)
     82 FORMAT(3F5.1,3E10.2)
        READ(11,83) ((A(I,J),I#1,13),J#1,3)
     83 FORMAT(9F7.1)
        READ(11,84) L
     84 FORMAT(I4)
        IF(L) 35,35,34
     34 READ(11,85) SK(1)
     85 FORMAT(E10.1)
        READ(11,86) (SK(I),I#2,14)
     86 FORMAT(8F10.1)
     35 CONTINUE
        WRITE(15,51) N
        WRITE(15,52) CL,(MT(I),I#1,2)
        DO 5 J#1,3
        C(13,J)#A(13,J)
        DO 6 I#1,12
        C(I,J)#A(I,J)
        A(I,J)#((A(1,J)-A(13,J))※FLOAT(I-1))/12.0+A(I,J)
      6 CONTINUE
        VA(J)#((A(1,J)-A(7,J)+0.8666※(A(2,J)-A(6,J)-A(8,J)+
       1A(12,J))+0.5※(A(2,J)-A(5,J)-A(9,J)+A(11,J)))※SN(J)※
       2D(J)※※3.0)/6.0/G
        VB(J)#((A(4,J)-A(10,J)+0.8666※(A(3,J)+A(5,J)-A(9,J)-
       1A(11,J))+0.5※(A(2,J)+A(6,J)-A(8,J)-A(12,J)))※SN(J)※
       2D(J)※※3.0)/6.0/G
        SA#0.0
        SD(J)#0.0
        DO 40 I#1,12
        A(I,J)#A(I,J)/G※SN(J)※D(J)※※3.0
        SA#SA+A(I,J)/12.0
     40 CONTINUE
        DO 12 I#1,12
        SD(J)#SD(J)+(ABS(SA+VA(J)※COS(30.0/57.296※FLOAT(I-1))+
       1VB(J)※SIN(30.0/57.296※FLOAT(I-1))-A(I,J)))※※2.0/12.0
     12 CONTINUE
        SD(J)#SQRT(SD(J))/SQRT((ABS(VA(J)))※※2.0+(ABS(VB(J)))
       1※※2.0)
      5 CONTINUE
        V(2,1)#VB(3)
        V(2,2)#VB(1)
        V(2,3)#VB(2)
        V(3,1)#VA(1)
        V(3,2)#VA(2)
        V(3,3)#VA(3)
```

Fig. 17a

```
      DO 13 J#1,3
      SD(4)#SD(1)
      SD(5)#SD(2)
      JPL2#J+2
      V(1,J)#V(2,J)*SD(J)/(SD(J)+SD(JPL2))+V(3,J)*SD(JPL2)/
     1(SD(J)+SD(JPL2))
      V(4,J)#(V(2,J)+V(3,J))/2.0
      V(5,J)#ABS(V(2,J)-V(3,J))/2.0
13    CONTINUE
      IP#0
      DPS#ABS(ST(2,1))
      DO 14 I#1,4
      VTEMP#V(I,2)
      V(I,2)#VTEMP*SIN(DPS/57.296)+V(I,3)*COS(DPS/57.296)
      V(I,3)#-VTEMP*COS(DPS/57.296)+V(I,3)*SIN(DPS/57.296)
14    CONTINUE
      STS#ST(1,1)/57.296
      DO 18 I#1,4
      VTEMP#V(I,1)
      V(I,1)#ST(2,1)/ABS(ST(2,1))*(-VTEMP*COS(STS)-V(I,2)*
     1SIN(STS))*ST(1,1)/ABS(ST(1,1))
      V(I,2)#ST(2,1)/ABS(ST(2,1))*(VTEMP*SIN(STS)-V(I,2)*
     1COS(STS))*ST(1,1)/ABS(ST(1,1))
18    CONTINUE
19    DRD#ATAN(V(1,3)/SQRT((ABS(V(1,1)))**2.0+(ABS(V(1,2)))
     1**2.0))
70    IF(DRD) 71,72,73
71    P#-ATAN(2.0*COS(DRD)/SIN(DRD))
      GO TO 74
72    DRD#DRD+0.0001
      GO TO 70
73    P#3.1416-ATAN(2.0*COS(DRD)/SIN(DRD))
74    DRD#DRD*57.296
      SLAT#SLAT*57.296
      ISN#0
26    IF(V(1,1)) 22,23,24
22    DRS#-ATAN(V(1,2)/V(1,1))+DCL/57.296
      IF(ABS(DRS)-1.5708) 41,41,42
41    SPHI#SIN(SLAT)*COS(P)+COS(SLAT)*SIN(P)*COS(DRS)
      ISN#ISN+1
75    PHI#ATAN(SPHI/SQRT(1.0-(ABS(SPHI))**2.0))
      SDLON#SIN(P)*SIN(DRS)/COS(PHI)
      DLON#ATAN(SDLON/SQRT(1.0-(ABS(SDLON))**2.0))
      CPC#SIN(SLAT)*SIN(PHI)+COS(SLAT)*COS(PHI)*COS(DLON)
      COSP#COS(P)
      IF(ABS(CPC-COSP).LE.0.01) GO TO 45
      DLON#(DLON/ABS(DLON))*(3.1416-ABS(DLON))
45    VLON#SLON-DLON*57.296
      DRS#DRS*57.296
      PHI#PHI*57.296
      SLAT#SLAT*57.296
      IF(1-ISN) 76,76,77
76    WRITE(15,53)DRS,DRD,ST(1,1),ST(2,1)
      GO TO 25
42    DRS#(DRS/ABS(DRS))*(3.1416-ABS(DRS))
```

Fig. 17b

```
      GO TO 43
   23 V(1,1)#V(1,1)+0.0001
      GO TO 26
   24 DRS#ATAN(V(1,2)/V(1,1))-DCL/57.296
      IF(1.5708-ABS(DRS)) 44,43,43
   43 SPHI#SIN(SLAT)*COS(P)-COS(SLAT)*SIN(P)*COS(DRS)
      GO TO 75
   44 DRS#(DRS/ABS(DRS))*(3.1416-ABS(DRS))
      GO TO 41
   77 WRITE(15,54) DRS,DRD,ST(1,1),ST(2,1)
   25 DO 31 J#1,3
      V(5,J)#ABS(V(2,J)-V(3,J))/2.0
   31 CONTINUE
      IF(V(4,1)) 38,39,38
   39 V(4,1)#V(4,1)+0.0001
   38 ES# ABS(ATAN(V(4,2)/V(4,1))-ATAN((V(4,2)+V(5,2))/
     1(V(4,1)-V(5,1))))*57.296
      ED#ABS(DRD-ATAN((V(4,3)+V(5,3))/SQRT((ABS(V(4,1)-
     1V(5,1)))**2.0+(ABS(V(4,2)-V(5,2)))**2.0))*57.296)
      WRITE(15,55) ES,ED
      WRITE(15,64) PHI,VLON,SLAT,SLON,DCL
      IF(IP-1) 28,29,29
   28 DO 27 I#1,4
      STS#ST(1,2)/57.296
      ASTS#ABS(STS)
      VTEMP#V(I,1)
      V(I,1)#VTEMP*SIN(ASTS)+V(I,2)*COS(ASTS)*STS/ASTS
      V(I,2)#V(I,2)*SIN(ASTS)-VTEMP*COS(ASTS)*STS/ASTS
      DPS#ST(2,2)/57.296
      VTEMP#V(I,1)
      V(I,1)#VTEMP*COS(DPS)-V(I,3)*SIN(DPS)
      V(I,3)#VTEMP*SIN(DPS)+V(I,3)*COS(DPS)
      VTEMP#V(I,1)
      V(I,1)#-V(I,2)*COS(ASTS)*ASTS/STS+VTEMP*SIN(ASTS)
      V(I,2)#VTEMP*COS(ASTS)*ASTS/STS+V(I,2)*SIN(ASTS)
   27 CONTINUE
      ST(1,1)#ST(1,2)
      ST(2,1)#ST(2,2)
      IP#IP+1
      GO TO 19
   29 S#SQRT((ABS(V(1,1)))**2.0+(ABS(V(1,2)))**2.0+
     1(ABS(V(1,3)))**2.0)
      WRITE(15,56) S
      WRITE(15,57)(SD(J),J#1,3)
      WRITE(15,58)((V(J,I),I#1,3),J#1,3)
      WRITE(15,59)(SN(I),I#1,3)
      WRITE(15,60)(D(I),I#1,3),G
      WRITE(15,61)((C(I,J),I#1,13),J#1,3)
      IF(L) 36,36,37
   37 WRITE(15,62) SK(1)
      WRITE(15,63) (SK(I),I#2,14)
   51 FORMAT(1H1,5X,7HJOB NO.,2X,I5)
   52 FORMAT(1H0,10HSAMPLE NO.,2X,A8/1H0,5HSTART,2X,I10,1X,
     12HTO,1X,I6)
```

Fig. 17c

```
53 FORMAT( 1H0, 42HNORTH POLE DIRECTION STRIKE DIP (W+,E-)  N,
  12F7.2,/1H ,42HSTRIKE DIP OF SAMPLE OR BED (W+,E-)       N,
  22F7.2)
54 FORMAT( 1H0, 42HNORTH POLE DIRECTION STRIKE DIP (W+,E-)  S,
  12F7.2,/1H ,42HSTRIKE DIP OF SAMPLE OR BED (W+,E-)       S,
  22F7.2)
55 FORMAT( 1H ,42HERROR ANGLE OF STRIKE AND DIP (+-DEGREE)  ,
  12F7.2)
56 FORMAT( 1H0, 32HMAGNETIC INTENCITY (OE*CM**3/CC),10X,
  11PE11.4)
57 FORMAT( 1H0, 32HSTANDARD DEVIATION (N-E,E-D,D-N)/1H ,25X,
  13F12.5)
58 FORMAT( 1H0, 44HLAST DIRECTION VECTOR (OE*CM**3/CC,SN WE UD)
  1,/1H ,25X,3(3(1PE12.4)/1H ))
59 FORMAT( 1H0, 40HSENS OF MAGNETMETER (OE/MM,N-E,E-D,D-N),/
  11H ,25X,3(1PE12.4))
60 FORMAT( 1H0, 25HDISTANS  (CM,N-E E-D D-N),3F12.2/1H0,
  121HVOLUME OF SAMPLE (CC),6X,F10.2)
61 FORMAT( 1HO/1H0, 23HDATA OF MESUREMENT (MM),/1H ,3HN-E,/
  11H ,9F8.2/1H ,4F8.2/1H ,3HE-D,/1H ,9F8.2/1H ,4F8.2/1H ,
  23HD-N,/1H ,9F8.2/1H ,4F8.2)
62 FORMAT( 1HO/1H0, 25HDATA OF SENS TEST (OE,MM),/1H ,1PE11.4)
63 FORMAT( 1H ,9F8.2/1H ,4F8.2)
64 FORMAT( 1H0, 42HVIRTUAL MAGNETIC POLE POSITION LAT,LON(NE),
  12F7.2/1H ,38HSAMPLING POSITION AND DECLINATION(W+) ,
  23F7.2)
36 GO TO 1
 2 STOP
   END
```

Fig. 17d

Fig. 17 Program of electronic computer for analysis of paleomagnetic data.

where, V_{NS}, V_{EW} and V_{UD} are components of north-south, east-west and up-down directions, respectively.

Error angles of declination ED, and of inclination EI, are calculated from the differences of two components in the same direction:

$$\tan(I-EI) = \frac{V_{UD}+\Delta V_{UD}}{\sqrt{(V_{EW}-\Delta V_{EW})^2+(V_{NS}-\Delta V_{NS})^2}}$$

$$\tan(D-ED) = \frac{V_{EW}+\Delta V_{ED}}{V_{NS}+\Delta V_{NS}}$$

where, V is the average value of components of the same direction and ΔV is the difference of the components of the same direction.

The virtual magnetic north pole position (ϕ', λ') is calculated from declination D, inclination I, latitude and longitude of sampling position (ϕ_0, λ_0):

$$\cot P = (1/2)\tan I$$

$$\sin\phi' = \sin\phi_0\cos P + \cos\phi_0\sin P\cos D$$

$$\sin(\lambda_0-\lambda') = \sin P\sin D/\cos\phi'$$

Flow chart of this calculations and program of electronic computor are shown in Figs. 16 and 17.

REFERENCES

Aoki, N., 1963, Pliocene and Pleistocene Foraminifera from along the Yoro River, Boso Peninsula — vertical faunal change. *Tokyo Kyoiku Daigaku, Sci. Rep., sec. C*, v. 8, no. 78, p. 203–227.

————, 1968, Benthonic foraminiferal zonation of the Kazusa Group, Boso Peninsula. *Palaeont. Soc. Japan, Trans. Proc. N.S.*, no. 70, p. 238–266.

Asano, K., 1938, Foraminiferal fauna from Boso Peninsula. *Tohoku Univ., Inst. Geol. Pal., Contr.*, no. 31, p. 57–96.

Berggren, W.A., 1969, Cenozoic chronostratigraphy, planktonic foraminiferal zonation and the radiometric time scale. *Nature*, v. 224, no. 5224, p. 1072–1075.

Black, D.I., 1967, Cosmic ray effects and faunal extinctions at geomagnetic field reversals. *Earth Planet. Sci. Letters*, v. 3, no. 3, p. 225–263.

Bradshow, J.S., 1959, Ecology of living planktonic Foraminifera in the north and equatorial Pacific Ocean. *Cushman Found. Foram. Res., Contrib.*, v. 10, pt. 2, p. 25–64.

Cox, A., 1968, Lengths of geomagnetic polarity intervals. *Jour. Geophys. Res.*, v. 73, no. 10, p. 3247–3260.

————, 1969, Geomagnetic reversals. *Science*, v. 163, no. 3864, p. 237–245.

———— and Dalrymple, G.B., 1967, Statistical analysis of geomagnetic reversal data and the precision of Potassium-Argon dating. *Jour. Geophys. Res.*, v. 72, no. 10, p. 2603–2614.

————, Doell, R.R. and Dalrymple, G.B., 1963, Geomagnetic polarity epochs and Pleistocene geochronometry. *Nature*, v. 198, no. 4885, p. 1047–1051.

Craig, H., 1965, The measurement of oxygen isotope paleotemperatures. *In* Stable isotopes in oceanographic studies and paleotemperatures, p. 3–24, *Consiglio Nazionale delle Ricerche*, Pisa.

Doell, R.R. and Cox, A., 1967, Analysis of alternating field demagnetization equipment. *In* Collison, D.W., Greer, K.M. and Runcorn, S.K., Methodes in paleomagnetism, p. 241–253, *Elsevier*, Amsterdam.

Epstein, S., Buchsbaum, R., Lowenstam, H.A. and Urey, H.C., 1953, Revised carbonate-water isotopic temperature scale. *Geol. Soc. Amer., Bull.*, v. 64, no. 11, p. 1315–1326.

Hanzawa, S., 1931, On some Miocene rocks with *Lepidocyclina* from the Izu and Boso Peninsulas. *Tohoku Imp. Univ., Sci. Rep., 2nd ser. (Geol.)*, v. 12, no. 2, 159–170

Harman, H.H., 1967, Modern factor analysis. 2nd ed., 474p. *Univ. Chicago Press*, Chicago.

Harrison, C.G.A., 1968, Evolutionary processes and reversals of the earth's magnetic field. *Nature*, v. 217, no. 5123, p. 46–47.

Hatai, K., 1958, Boso Peninsula. *Jub. Publ. Commen. Prof. H. Fujimoto, 60th Birthday*, p. 183–201.

Hays, J.D. and Opdyke, N.D., 1967, Antarctic Radiolaria, magnetic reversals and climatic changes. *Science*, v. 158, no. 3804, p. 1001–1011.

————, Saito, T., Opdyke, N.D. and Burckle, L.H., 1969, Pliocene-Pleistocene sediments of the equatorial Pacific, their paleomagnetic, biostratigraphic, and climatic record. *Geol. Soc. Amer., Bull.*, v. 80, no. 8, p. 1481–1514.

Hirayama. J. and Suzuki, Y., 1968, Analysis of layers – An example in flysch-type alternations. *Earth Science (Chikyu Kagaku)*, v. 22, no. 2, p. 43–62.

Horibe, Y., 1966, Measurement of isotopic ratio of light elements. *Mass Spectroscopy*, v. 14, no. 3, p. 113–120.

———— and Oba, T., 1969, Paleotemperatures of deep-sea cores from the Indian Ocean by oxygen isotope method. *Fossils, Special Issue*, no. 1, p. 21–30.

————, ———— and Niitsuma, N., 1969, Relationship between water temperature and oxygen isotopic ratio. *Fossils, Special, Issue*, no. 1, p. 15–20.

Imbrie, J. and Purday, E.G., 1962, Classification of modern Bahamian carbonate sediments. *In* Classification of carbonate rocks, *Amer. Assoc. Petrol. Geol., Mem.*, no. 1, p. 253–272.

Kawai, N., 1951, Magnetic polarization of Tertiary rocks in Japan. *Jour. Geophys. Res.*, v. 56, no. 1, p. 73–79.

Mitsunashi, T., Yasukuni, N. and Shimada, Y., 1959, Stratigraphical section of the Kazusa Group along the shores of the Rivers Yoro and Obitsu. *Geol. Surv. Japan, Jour.*, v. 10, no. 2, p. 83–89.

————, Yazaki, N., Shimada, T., Ono, A., Yasukuni, N., Makino, T., Shinagawa, T., Fujiwara, K. and Kamata, K., 1961, "Futtsu Otaki", Geological maps of the oil and gas field of

Japan, no. 4, *Geol. Surv. Japan.*

Motomura, I., 1932, Statistical method in animal association. *Zool. Mag., Japan*, v. 44, no. 528, p. 379–398.

Nagata, T., 1961, Rock magnetism. 2nd ed. 350p. *Maruzen*, Tokyo.

Nakagawa, H., 1962, Strctural growth of the Kanto tectonic basin. *Tohoku Univ., Sci. Rep., 2nd ser. (Geol.), Spec. Vol.*, no. 5, p. 373–393.

————, 1965, Pleistocene sea levels along the Pacific coast of Japan. *Tohoku Univ., Sci. Rep., 2nd ser. (Geol.)*, v. 37, no. 1, p. 31–39.

————, Niitsuma, N. and Hayasaka, I., 1969, Late Cenozoic geomagnetic chronology of the Boso Peninsula. *Geol. Soc. Japan, Jour.*, v. 75, no. 5, p. 267–280.

————, ———— and Elmi, C., 1971, Pliocene and Pleistocene magnetic stratigraphy in le Castella area, southern Italy— a preliminary report. *Quat. Res.*, v. 1, no. 3, (in press).

Niitsuma, N., 1968, Analysis of the benthonic foraminiferal community. *Fossils*, no. 16, p. 25–33.

————, 1970, Some geomagnetic stratigraphical problems in Japan and Italy. *Jour. Mar. Geol.*, v. 6, no. 2, p. 99–112.

————, 1971, Automatic grain-size analyser for sedimentological investigation. *Tohoku Univ., Inst. Geol. Pal., Contr.*, no. 72, (in press).

———— and Mekata, Y., 1971, The analysis of the sediments of Mutsu Bay by the automatic grain-size analyser. *ibid.* no. 72, (in press).

———— and ————, 1971, The analysis of the sediments of continental shelf and slope along the Pacific coasts of Honshu, Japan. *Geol. Soc. Japan, Jour.*, (in press).

————, Sakai, T. and Hattori, M., 1971, Statistical analyses of populations by electronic computer. *Tohoku Univ., Sci. Rep., 2nd ser. (Geol.)*, v. 43, p. 41–58.

Ninkovich, D., Opdyke, N., Heezen, B.C. and Foster, J.H., 1966, Paleomagnetic stratigraphy, rates of deposition and tephrachronology in north Pacific deep-sea sediments. *Earth Planet. Sci. Letters*, v. 1, no. 6, p. 476–492.

Nobuhara, H. and Numata M., 1954, Essentials of the law of geometrical progression — Studies on the fundamental structure of biological populations. *Soc. Plant Ecol., Bull.*, v. 3, no. 4, p. 180–185.

Oba, T., 1969, Biostratigraphy and isotopic paleotemperature of some deep-sea cores from the Indian Ocean. *Tohoku Univ., Sci. Rep., 2nd ser. (Geol.)*, v. 41, no. 2, p. 129–196.

Ogose, S., 1961, Molluscan fossils from the Zizodo Sand and the Yabu Sand and Gravel, Tiba Preferecture, south Kanto, Japan. *Geol. Soc. Japan, Jour.*, v. 67, no. 785, p. 105–127.

Opdyke, N.D., Glass, B., Hays, J.D. and Foster, J., 1966, Paleomagnetic study of Antarctic deep-sea cores. *Science*, v. 154, no. 3747, p. 349–356.

Petrova, G.N., 1965, On validity of paleomagnetic data and transitional regime of geomagnetic field. *Jour. Geomag. Geoele.*, v. 17, no. 3–4, p. 425–434.

Preston, F.W., 1948, The commonness and rarity of species. *Ecol.*, v. 29, no. 3, p. 254–283.

Reid, J.L., Jr., 1965, Intermediate waters of the Pacific Ocean. *In* the Johns Hopkins Oceanographic studies, *Johns Hopkins Press*, Baltimore.

Saito, T., 1963, Miocene planktonic Foraminifera from Honshu, Japan. *Tohoku Univ., Sci. Rep., 2nd ser. (Geol.)*, v. 35, no. 2, p. 123–209.

Smith, P.J., 1967a, The intensity of the ancient geomagnetic field — a review and analysis. *Geophys. Jour.*, v. 12, p. 321–362.

————, 1967b, Ancient geomagnetic field intensities, 1, Historic and archeological data — Sets H1–H9. *Geophys. Jour.*, v. 13, p. 417–419.

————, 1968, Ancient geomagnetic field intensities geological data — Sets G1–G2; Historic and archeological data — Sets H10–H13. *Geophys. Jour.*, v. 13, p. 483–486.

Ujiié, H., 1968, Distribution of living planktonic Foraminifera in the southeast Indian Ocean. *National Sci. Mus., Bull.*, v. 11, no. 1, p. 97–125.

Waddington, C.J., 1967, Paleomagnetic field reversals and cosmic radiation. *Science*, v. 158, no. 3803, p. 913–915.

Whittaker, R.H., 1965, Dominance and diversity in land plant communities. *Science*, v. 147, no. 3655, p. 250–260.